Quantifying the relative influence of coastal foredune growth factors on the U.S. Mid-Atlantic Coast using field observations and the process-based numerical model Windsurf

Paige A. Hovenga[1]*, Peter Ruggiero[2], Michael Itzkin[3], Katya R. Jay[4], Laura Moore[3], Sally D. Hacker[4]

[1] School of Civil and Construction Engineering, Oregon State University, Corvallis, Oregon, USA

[2] College of Earth, Ocean, and Atmospheric Sciences, Oregon State University, Corvallis, Oregon, USA

[3] Department of Geological Sciences, University of North Carolina at Chapel Hill, Chapel Hill, North Carolina, USA

[4] Department of Integrative Biology, Oregon State University, Corvallis, Oregon, USA

*Corresponding Author: Paige Hovenga, email address: paige.hovenga@gmail.com, phone: (954) 404-2588, 101 SW 26th St., Corvallis, Oregon, USA 97331. Now at: Woods Hole Oceanographic Institution.

Highlights

- Pre-existing beach-dune morphology had the largest influence on dune growth type.
- Exposure to the dominant wave direction led to increased dune volume.
- Higher minimum vegetation elevation and finer sand resulted in taller dunes.
- Minimum vegetation elevation influenced dune growth more than sand grain size.

Abstract

Coastal dunes provide many ecosystem services including protection of infrastructure from wave overtopping and habitat for native species. Foredunes grow at different rates and assume different forms (i.e., short and wide to tall and narrow) depending on a range of factors including pre-existing beach and dune morphology, wind, wave, and water levels, sediment grain size, and vegetation characteristics, yet the relative importance of these factors on foredune growth is understudied. Here, we quantify foredune evolution (2016-2019) and explore the relative influence of a suite of metocean, sedimentary, and ecological factors for dune growth on three barrier islands in the U.S. North Carolina Outer Banks (Cape Lookout National Seashore). We incorporate observed and hindcast wind, wave, and water level data into the process-based, coupled beach-dune evolution model, Windsurf, to explore the relative contribution of factors likely to influence foredune growth at the annual timescale (2016-2017). Our cross-shore topographic profile observations show varied interannual foredune change rates and characteristics, including horizontal retreat and progradation at the dune toe and vertical erosion and accretion at the dune crest. Model results indicate that, of the factors explored, pre-existing morphology had the greatest influence on the type of foredune growth that occurred (i.e., incipient dune development, widening of the dune, and/or vertical accretion), which dramatically altered the final shape of the dune. Variations in wind and wave climates were associated with the relative contribution of marine- and aeolian-driven bed elevation changes and were particularly influential during storms. In addition, increases in the minimum elevation of vegetation on the dune profile (analogous to the cross-shore distance between the shoreline and

established vegetation line, i.e., the vegetation limit, as coined by Duran and Moore, 2013) increased dune crest height and dune volume. Moreover, variations in the minimum vegetation elevation resulted in a larger range of dune crest elevations and dune volumes than differences in the median sand grain size. We suggest that insights into the relative influence of metocean, sedimentary, and ecological factors to dune growth can assist in the development of practical coastal management strategies.

Keywords

Coastal foredune growth, dune dynamics, ecomorphodynamics, coupled beach-dune modeling, sediment transport, accretion, progradation

1. Introduction

Coastal dunes provide a range of regulating, provisioning, cultural, and supporting ecosystem services including coastal hazard protection, carbon sequestration, living spaces, historical heritage, tourism, habitat for flora and fauna, and nutrient cycling (Barbier et al., 2011; Martínez and Psuty, 2004; Nordstrom et al., 1989; Sudmeier-Rieux et al., 2019). Dunes form, develop, and recover from storms via complex ecomorphodynamic processes produced by the interactions and feedbacks between metocean, sedimentary, and ecological factors (Biel et al., 2019; Charbonneau et al., 2022; Corenblit et al., 2011; Durán and Moore, 2013; Hacker et al., 2019; Hesp, 1989; Hesp et al., 2019; Jay et al., 2022; Keijsers et al., 2016; Woodhouse, 1978; Yousefi Lalimi et al., 2017; Zarnetske et al., 2015). Moreover, the rates and types of coastal dune growth, including incipient dune development, widening of the dune, and/or vertical accretion, are dependent on pre-existing nearshore, beach, and dune morphology (Godfrey, 1977). Understanding the relative influence of factors influencing dune development is important for predicting exposure to coastal hazards, improving coastal engineering design, and informing decisions for resilient adaptation strategies (Gracia et al., 2018; Nordstrom et al., 1989) .

Dune growth is primarily associated with aeolian transport of sediment from the beach to the dune (Goldsmith, 1978). Controls on aeolian sediment transport include the wind climate (i.e., velocity, direction, and duration) and fetch length (determined by beach width), as well as the moisture content, sediment grain size distribution, and topography of the beach (Bauer et al., 2009; Hoonhout and de Vries, 2016; Walker, 2020; White and Tsoar, 1998). Transport is typically modeled using a threshold velocity approach (Bagnold, 1941), whereby wind velocities exceeding a threshold will have the capacity to entrain sediment. Cross-shore transport of sediment is highest for shore-normal winds and is reduced for oblique winds (i.e., the cosine effect); however, oblique winds result in increased fetch lengths between the waterline and dunes (Bauer and Davidson-Arnott, 2003; Davidson-Arnott et al., 2018). Additionally, the concept of duration-limited wind events has been proposed (Delgado-Fernandez and Davidson-Arnott, 2011), where a duration factor is used to regulate the amount of ‘geomorphic work’ done by grouped wind events. The fetch length and sediment transport rate are further modulated by the moisture content of the beach, which is a function of nearshore processes (e.g., tidal fluctuations and runup) and rainfall events (Bauer et al., 2009).

Beach grain size distribution is another important factor that can govern supply and transport of sand to the dune. Fine sands are more easily transported, leaving coarser-grained lag on the beach surface (Bagnold, 1941; Wolner et al., 2013). Areas of the beach that lack finer sands below the beach surface, and do not experience hydraulic mixing from wave action, can result in lower rates of sand transport across the beach and thus limit sediment supply to the dune (Hoonhout, 2020; Hoonhout and de Vries, 2016). Additionally, coarser grain sizes will increase the surface roughness length, thus reducing the threshold wind velocity (Bagnold, 1941; Belly, 1964; Field and Pelletier, 2018).

Topographic characteristics such as beach slope, presence or absence of berms and cusps, and dune structures themselves significantly interact with wind velocities and alter bed shear stresses (Bauer et al., 1996; Jackson et al., 2013; Jackson and Hunt, 1975; Sherman and Bauer, 1993; Walker and Hesp, 2013; Walker, 2020). Similarly, dune vegetation increases localized drag and reduces bed shear stress, resulting in sediment deposition (Charbonneau and Casper, 2018; Hesp et al., 2019; Hong et al., 2019; Liu et al., 2018; Olson, 1958a; Walker and Hesp, 2013; Zarnetske et al., 2012). Ecological characteristics of dunes such as vegetation abundance and species composition are important determinates of dune morphology and evolution, given the dual role of plants in dune-building (sand accretion) and stabilization (minimizing sand loss) (Arens et al., 2001; Biel et al., 2019; Bonte et al., 2021; Bryant et al., 2019; Charbonneau et al., 2021, 2017; Durán and Moore, 2013; Esler, 1970; Hacker et al., 2019, 2012; Hesp, 1989; Jay et al., 2022; Keijsers et al., 2016; Olson, 1958b; Seabloom et al., 2013).

Dune growth is also a function of marine processes such as waves, currents, and wave runup, which interact with the beach-dune profile and influence sediment transport gradients (Cohn et al., 2018; Hesp and Smyth, 2016; Sherman and Bauer, 1993; Short and Hesp, 1982). Although marine processes clearly can have significant erosional impacts on coastal foredunes, particularly during storm events (Castelle et al., 2017; Komar et al., 2001; Masselink et al., 2016; Sallenger, 2000), recent studies have shown that marine-driven sediment transport can also be a significant contributor to dune growth (Cohn et al., 2019a, 2019b; Moulton et al., 2021). For specific hydrodynamic states, i.e., high still water level and/or energetic wave periods, dune growth rates driven by marine processes can be an order of magnitude larger than dune growth rates driven by aeolian processes (Cohn et al., 2019a). In addition, wave climate (i.e., wave height, period, and direction) can alter morphology, including the foreshore beach slope, beach width, dune toe elevation, and dune crest elevation (Castelle et al., 2019; Cohn et al., 2019b; Short and Hesp, 1982; Splinter et al., 2018). Likewise, morphology affects wave runup processes and ultimately the effect of total water level on dune evolution (Cohn et al., 2021; Gomes da Silva et al., 2020; Holman and Sallenger, 1985; Sallenger, 2000; Stockdon et al., 2006). Alongshore varying wave energy also drives gradients in longshore sediment transport, influencing beach sediment budgets and ultimately affecting foredune growth (Miot da Silva et al., 2012; Psuty, 1988).

Previous studies have used field observations to explore the relative contribution of various geological and ecological factors important to dune morphology and growth. For example, research on the U.S. Pacific Northwest coast (Biel et al., 2019) and the North Carolina Outer Banks (Jay et al., 2022) has shown that shoreline change rate and beach slope were significant factors in foredune morphology and its change, while dune grass density and species identity explained less variability. The relative influence of these factors has also been shown to depend on the timescales over which they are considered. For example, beach sand supply was found to explain more variation in foredune morphology at shorter timescales (i.e., annual) while beach grass density explained more variation at longer timescales (i.e., decadal) suggesting that sand supply and vegetation feedbacks on dune morphology take many years to develop (Zarnetske et al., 2015).

Field-based observational and experimental studies have revealed the importance of multiple factors to dune evolution, but they are typically bound by the site-specific combination of factors and relatively short time scales. Process-based, beach-dune models provide the means for manipulating the various factors important to dune morphology in a controlled manner. State-of-the-art, beach-dune models couple nearshore morphodynamic and dune evolution processes to holistically simulate the full coastal profile. Such models, including XBeach-Duna (Roelvink and Costas, 2019), DUBEVEG (Keijsers et al., 2016), and Windsurf (Cohn et al., 2019a) provide platforms to enhance our knowledge of the interdependent physical factors controlling coastal dune evolution. For example, Windsurf couples XBeach (Roelvink et al., 2009), Aeolis (Hoonhout and de Vries, 2016), and the Coastal Dune Model (Durán and Moore, 2013) to coevolve the nearshore, beach, and dune in response to both subaqueous and subaerial sediment transport (Cohn et al., 2019a; Itzkin et al., 2022). Windsurf can be used to test a range of boundary conditions related to ecomorphodynamic processes to explore the relative influence of different factors on foredune morphology and its change (Ruggiero et al., 2019). Windsurf was initially developed and tested with reasonable skill for a wide, dissipative beach on the west coast of the U.S. over a one-year period (Cohn et al., 2019a). More recently, Windsurf has been used to reproduce hindcasts of beach evolution and vertical dune growth over a one-year period at two field sites on Bogue Banks, a barrier island in North Carolina, U.S. (Itzkin et al., 2022). The study of Itzkin et al. (2022) included management scenarios for dunes with and without sand fences.

In this study, we initially quantify dune morphology and its interannual change along Cape Lookout National Seashore (CALO, North Carolina, USA). We then investigate the relative influence of factors that are likely to affect rates and types (i.e., incipient dune development, widening of the dune, and/or vertical accretion) of foredune growth using Windsurf. Our specific research questions are:

1) What are the observed temporally and spatially varying rates and characteristics of foredune morphological change along our study region?

2) What are the relative contributions of key factors, including pre-existing morphology, environmental wind and hydrodynamic forcing conditions, sediment grain size distribution, and minimum vegetation elevation, to foredune growth in this region?

We first quantified foredune changes using annually collected in-situ geomorphological measurements from 2016-2019. These data, along with in-situ ecological observations and environmental conditions (e.g., water level, wave, and wind data) compiled from hindcast and observed data, were incorporated into Windsurf and used to produce a one-year hindcast of dune growth at a diagnostic field site. We then used the calibrated model to explore and quantify the relative influence of pre-existing morphology, environmental forcing conditions, sediment, and ecological characteristics at the annual timescale via two distinct numerical modeling experiments: one using observations from four field sites along CALO that exhibited different rates and types of foredune growth and one using the full range of foredune growth factors observed within our entire study area. We calculated changes from the initial and final modeled response variables (i.e., dune toe elevation, dune crest elevation, and sediment volume above a contour) to evaluate how different factors within the model affected dune growth. This work aims to improve our understanding of foredune growth and recovery processes and provides insights for modeling coastal change, predicting coastal hazard vulnerability, and guiding coastal adaptation strategies including dune grading, dune grass planting, and beach nourishment projects.

2. Methodology

2.1. Study Area, Field Observations, and Other Datasets

Cape Lookout National Seashore (CALO) is located in North Carolina on the U.S. Atlantic Coast and consists of three barrier islands: Shackleford Banks (SHB), South Core Banks (SCB), and North Core Banks (NCB) (Figure 1). This region was established as a National Seashore in 1966 and is managed by the U.S. National Park Service. As such, CALO is minimally impacted by humans compared to more developed areas on the Outer Banks barrier islands. The CALO coastline exhibits spatial variability in beach and dune morphology, wind and wave climate, sediment characteristics, and dune grass composition and density, making it ideal to investigate for our study (Dolan and Lins, 1985; Godfrey, 1977, 1976; Goldstein et al., 2018; Hacker et al., 2019; Hovenga et al., 2021, 2019; Jay et al., 2022; Riggs and Ames, 2007; Stockdon and Thompson, 2007).

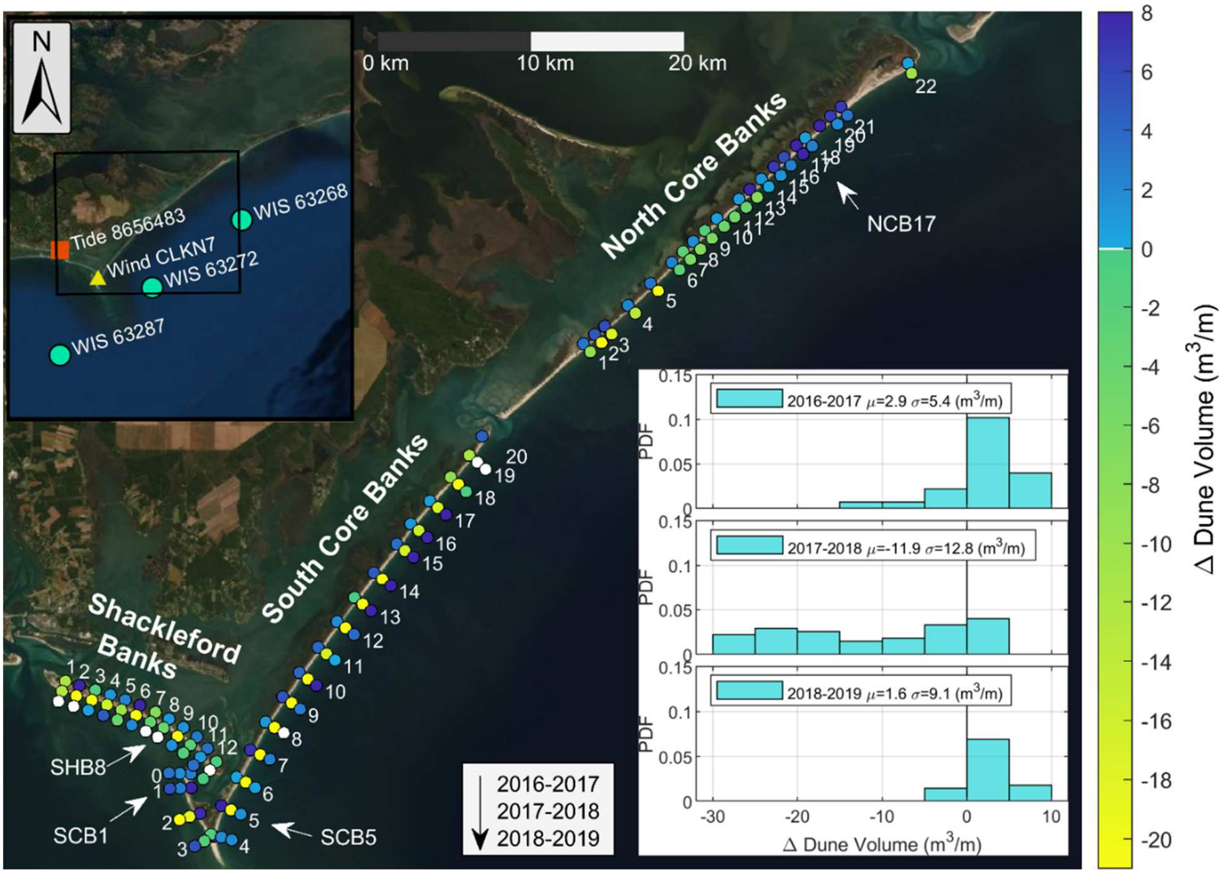

Figure 1. Cape Lookout National Seashore (North Carolina, USA) is comprised of three barrier islands: Shackleford Banks (SHB), South Core Banks (SCB), and North Core Banks (NCB). Markers indicate the 55 field sites (1-12 on SHB, 0-20 on SCB, and 1-22 on NCB) where topographic, sediment and vegetation data were collected. Marker colors indicate the interannual dune volume change (m^3/m) between surveys from 2016-2017, 2017-2018, and 2018-2019 moving seaward. Arrows show the locations of the SCB5, SHB8, SCB1, and NCB17 field sites. The bottom right plots show the probability density function (PDF), mean (μ), and standard deviation (σ) of the interannual volume change for all 55 field sites. The top left inset shows the locations of the National Oceanic and Atmospheric (NOAA) weather station (CLKN7), NOAA tide

gauge (8656483), and United States Army Corps of Engineers (USACE) Wave Information Studies (WIS) stations (63268, 63272, and 63287).

Beach and dune change along CALO was quantified using Real Time Kinematic Global Positioning System (RTK-GPS) techniques to measure annual in-situ topographic profiles along transects in the cross-shore direction. Additionally, surface sediment samples were collected at the dune toe and sieved to obtain grain size distributions. Vegetation characteristics were measured along the dune profile at each site, including grass density and a measure of minimum vegetation elevation, using the methods of Hacker et al. (2019) and Jay et al. (2022). These datasets were obtained at 55 field sites (12 on SHB, 21 on SCB, and 22 on NCB) annually in the fall of 2016-2019 (Figure 1; Table 1). NCB was not surveyed in 2019 due to the extensive overwash that occurred during Hurricane Dorian, resulting in unsafe field conditions. Foredune morphometrics, including the dune toe, crest, and heel, were extracted from the field measured cross-shore profiles using a manual delineation and interpretation approach (Fabbri et al., 2017; Lentz and Hapke, 2019). The dune volume was calculated between the seaward-most two-meter contour of the profile and the cross-shore location of the 2016 dune heel. All vertical references in this study are relative to the North American Vertical Datum of 1988 (NAVD88), which is 0.11 m above mean sea level (MSL) at the nearest tide gauge (Station: 8656483; NOAA, 2020a) (Figure 1). Note that total vertical uncertainty (i.e., arising from GPS, calibration, and repeatability errors combined in quadrature) associated with RTK-GPS methods is typically less than 8 cm (Ruggiero et al., 2005). The measured topography was merged with bathymetry from the National Centers for Environmental Information (NCEI) digital elevation model (DEM) to extend the profiles to approximately the nine-meter water depth contour (NOAA, 2016). Foreshore beach and shoreface slopes were calculated at MSL and the -6 m elevation contour, respectively, by fitting a linear regression to the profile at each contour location within ±5 m in the cross-shore direction. A definition sketch of the extracted beach and foredune morphometric features are provided in Hovenga et al. (2021).

Table 1. Collection dates and type of in-situ datasets collected at the three barrier islands: Shackleford Banks (SHB), South Core Banks (SCB), and North Core Banks (NCB) (Figure 1). Dataset types include cross-shore topographic profiles (topo), sediment samples collected at the dune toe, and vegetation measurements.

Dataset	Dates	Barrier Island	Dataset Type
2016	10/18-25/2016	SHB, SCB, NCB	Topo, sediment, vegetation
2017	10/14-20/2017	SHB, SCB, NCB	Topo, sediment, vegetation
2018	10/09-17/2018	SHB, SCB, NCB	Topo, vegetation
2019	11/10-13/2019	SHB, SCB	Topo, vegetation

Environmental conditions including wave height, period, and direction were acquired from USACE WIS hindcasts (U.S. Army Corps. of Engineers, 1997) (Figure 1). Wind speed and direction were acquired from the NOAA CLKN7 weather station (NOAA, 2020b) (Figure 1). Water level data was acquired from the NOAA tide gauge 8656483 (NOAA, 2020a) (Figure 1). The varying shoreline orientation within CALO influences the environmental forcing conditions experienced at each field site due to sheltering effects.

2.2. Windsurf Modeling Approach

We used the coupled numerical model Windsurf to simulate coastal profile evolution in response to marine- and aeolian-driven sediment transport (Cohn et al., 2019a). The modeling framework communicates model outputs (i.e., morphology, water levels, and bed shear stress) between the standalone model cores XBeach (release 1.23), Coastal Dune Model (CDM; release 1.0), and Aeolis (version 1.1.0). We first calibrated Windsurf for the SCB5 field site (Figure 1) using in-situ geomorphological and ecological observations combined with hourly water level, wave, and wind data. The model was then used to explore and quantify the relative influence of pre-existing morphology (i.e., topo-bathymetric profiles), environmental forcing conditions (i.e., wave and wind climate due to the varying shoreline orientation), sediment (i.e., median grain size, D_{50}, and distribution represented by D_{10}, D_{50}, and D_{50}) and ecological (i.e., minimum vegetation elevation) characteristics via two distinct numerical modeling experiments.

2.3. Model Calibration Procedure

Using observed conditions from 2016 to 2017 at field site SCB5 (Figure 1), we calibrated Windsurf at the annual scale by optimizing parameters related to the individual cores: Aeolis (i.e., the aeolian sediment transport coefficient, Cb) and XBeach (i.e., skewness factor, facSk, and asymmetry factor, facAs) (Figure 1; Table 2). We selected SCB5 because the high rate of vertical crest accretion and volumetric growth at this site encompassed the range of changes observed elsewhere (Section 3.1).

Table 2. Key calibration model parameters, range of tested values, and final calibrated values for the Windsurf model at the SCB5 field site (Figure 1). The model was calibrated using error metrics 1-8, and the error values for the final, one-year calibrated model are provided for each error metric.

Model Parameter	Model Core	Min Value	Increment	Max Value	Calibrated Value
Cb	Aeolis	0.1	0.1	0.3	0.3
facSk	XBeach	0	0.1	0.7	0.5
facAs	XBeach	0	0.1	0.7	0.2

Error Metrics	Error Value
(1) Dune volume (m^3/m)	-0.32
(2) Dune crest elevation (m)	-0.05
(3) Bed elevation at the 2016 dune toe cross-shore location (m)	0.16
(4) Root Mean Square Error (RMSE; m; computed between the observed 2017 seaward- and landward-most points)	0.16
(5) RMSE for the dune (m; measured between the 2016 dune toe cross-shore location and the observed 2017 landward-most point)	0.12
(6) Brier Skill Score (BSS [Murphy and Epstein, 1989; Sutherland et al., 2004]; computed between the observed 2017 seaward- and landward-most points)	0.96
(7) Bed elevation change at the 2.1 m depth (m)	1.18
(8) Bed elevation change at the 6.5 m depth (m)	-0.60

We ran 192 simulations using every combination of Cb, facSk, and facAs for the values listed in Table 2 while all other model parameter settings were set to default values. Note that a morphological acceleration factor (MORFAC) of 5 was used in XBeach after preliminary testing showed this value reduced model run time without significant change to model responses. Model responses were evaluated using values for the error metrics provided in Table 2. Error metrics 1-6 were calculated between the final 2017 modeled profile and 2017 observed profile. For example, error metric (1) dune volume is equal to the 2017 modeled dune volume minus the 2017 observed dune volume. Error metric 6 represents the Brier Skill Score (BSS) (Murphy and Epstein, 1989; Sutherland et al., 2004). Additionally, we computed the bed elevation change between the initial and final modeled profiles at two offshore depths (Error metrics 7 and 8); since no nearshore bathymetric change was measured for this study, these metrics were minimized for the smallest bed changes at the 2.1 and 6.5 m depths. The individual model runs were ranked by each error metric from best (largest BSS and smallest absolute minimum error for all other metrics) to worst (smallest BSS and largest absolute maximum error for all other metrics). We then computed two composite error scores, $CompErr_6$ and $CompErr_8$, using the following:

$$CompErr_n(m) = \sqrt{\frac{\sum_{i=1}^{n} rank\_err_i^2}{n}} \quad \text{(Eq 3.1)}$$

where $CompErr_n(m)$ is the composite error score for each model run, m. Each composite error score is computed using n number of error metrics and $rank\_err$ is the model simulation rank for each individual error metric, i (Table 2). $CompErr_8$ (computed from error metrics 1-8) was used to assess errors holistically across the nearshore, beach, and dune, while $CompErr_6$ (computed from error metrics 1-6) was used to finely assess the model performance across the beach and dune, which is the focus of this study. The final calibrated parameters Cb, facSk, and facAs were selected using the model simulation that scored best for both $CompErr_6$ and $CompErr_8$. Although we used a manual calibration approach, other more automated calibration methods such as those that utilize machine learning techniques (e.g., Goldstein and Moore, 2018 and Itzkin et al., 2022) may improve results but are beyond the scope of this study.

2.4. Modeling Experimental Design

We developed two 1D numerical modeling experiments to assess foredune responses to variations in the factors that are likely key influencers of foredune growth. Both modeling experiments focus on one year of data (2016–2017); this time period was selected because observations revealed significant alongshore variations in foredune growth rates and foredune growth types during this time window. For Experiment 1, the in-situ factors at four field sites (i.e., SCB5, SHB8, SCB1, and NCB17; Figure 1) were tested independently in Windsurf (Table 3). We chose these four sites because they exhibited different rates and types of foredune growth. Boundary conditions and all other model parameters remain unchanged from the calibrated SCB5, or ‘baseline model’ except for those shown in bold in Table 3. For example, Run 1.8 used the sediment size (D_{10}, D_{50}, D_{90}) measured at the SHB8 field site and all other dune growth factors remained unchanged from the baseline model.

Table 3. Modeling design for Windsurf Experiment 1. Run 1.1 is the calibrated SCB5 (baseline) model, which uses all the dune growth factors (pre-existing morphology, environmental conditions, sediment size, and minimum vegetation elevation) observed at the SCB5 field site. Runs 1.2-1.13 use different pre-existing morphology (Runs 1.2-1.4), environmental conditions (Runs 1.5-1.7), sediment size (Runs 1.8-1.10), and minimum vegetation elevation (Runs 1.11-13) boundary conditions that represent observations at the SHB8, SCB1, and NCB17 field sites. The bold text signifies which dune growth factors differ in each model run compared to the baseline model.

Run Number	**Pre-existing Morphology**	**Environmental Conditions**	**Sediment Size D_{10}, D_{50}, D_{90} (mm)**	**Minimum Vegetation Elevation (m)**

1.1 (Baseline)	SCB5	SCB5	0.16	0.25	0.38	3.0
1.2	**SHB8**	SCB5	0.16	0.25	0.38	3.0
1.3	**SCB1**					
1.4	**NCB17**					
1.5	SCB5	**SHB8**	0.16	0.25	0.38	3.0
1.6		**SCB1**				
1.7		**NCB17**				
1.8 (SHB8)	SCB5	SCB5	**0.20**	**0.31**	**0.53**	3.0
1.9 (SCB1)			**0.23**	**0.43**	**1.06**	
1.10 (NCB17)			**0.16**	**0.24**	**0.40**	
1.11 (SHB8)	SCB5	SCB5	0.16	0.25	0.38	**2.9**
1.12 (SCB1)						**2.1**
1.13 (NCB17)						**2.1**

In Experiment 2, we modeled foredune response with Windsurf from 2016-2017 using the full range of foredune growth factors (i.e., environmental forcing conditions dictated by the shore-normal angle, median grain size, and minimum vegetation elevation) observed within CALO (Table 4). We used the calibrated SCB5 model and only varied those parameters shown in Table 4. Shore-normal angles were measured in degrees using a nautical convention (i.e., the angle from where onshore is directed, measured clockwise from geographic North. For example, a shore-normal angle of 135 degrees would represent an onshore direction from the southeast to the northwest, a fairly typical shore-normal angle for NCB). For Runs 2.1-2.6, we tested a range of shore-normal angles from 100 to 250 degrees, increasing the shore-normal value by 30 degrees between each run (Table 4). These values represent the range of shore-normal angles measured at all 55 field sites within CALO (101 to 255 degrees; Table 4). For model Runs 2.1-2.6, we used the environmental conditions that would be experienced at a location for each specified shore-normal angle (Table 4; described in more detail below).

Table 4. Modeling design for Windsurf Experiment 2. We tested the full range of dune growth factors observed within CALO including the environmental conditions dictated by the shore-normal angle, median sediment grain size, and minimum vegetation elevation.

Run Number	Factors	Values	Observed CALO Range
2.1	Environmental Conditions (Shore-normal angle, degrees)	100	CALO Min = 101 CALO Max = 255 SCB5 = 115 SHB8 = 207 SCB1 = 249 NCB17 = 138
2.2		130	
2.3		160	
2.4		190	
2.5		220	
2.6		250	
2.7	Median Sediment Grain Size (D_{50}, mm)	0.15	CALO Min = 0.17 CALO Max = 0.44 SCB5 = 0.25 SHB8 = 0.31 SCB1 = 0.43 NCB17 = 0.24
2.8		0.20	
2.9		0.25	
2.10		0.30	
2.11		0.35	
2.12		0.40	
2.13		0.45	
2.14	Minimum Vegetation Elevation (m)	1.0	CALO Min = 0.9 CALO Max = 6.6 SCB5 = 3.0 SHB8 = 2.9 SCB1 = 2.1 NCB17 = 2.1
2.15		1.5	
2.16		2.0	
2.17		2.5	
2.18		3.0	
2.19		3.5	

Pre-existing morphology was implemented within the model as a 1D cross-shore profile. Cross-shore grid spacing varied from 20 m offshore to 1 m onshore of the -1 m contour. Increasingly finer grid resolution had minimal impact on the model results yet added significant computational time.

To account for the varying wind and wave environmental forcing conditions experienced at the SCB5, SCB1, NCB17, and SHB8 field sites, the onshore (shore-normal) angle was measured perpendicular to the average alongshore orientation at each of the field sites. The range of environmental forcing scenarios was implemented within Windsurf by pre-processing the input wind and wave directions to include the shore-normal components ± 90 degrees at SCB5, SCB1, NCB17, and SHB8 (Runs 1.1, 1.5-1.7 in Experiment 1) and for the shore-normal angles in Runs 2.1-2.6 in Experiment 2 (Table 4). Note, this filtering method did not violate the model coordinate system. These model runs were used to explore how the environmental conditions experienced at different locations within CALO may influence dune growth. Windsurf distinguishes between marine-driven (XBeach) and aeolian-driven (Aeolis) sediment transport which is explored within Experiment 2.

Sediment grain size characteristics are represented in the model core Aeolis by D_{10}, D_{50}, and D_{90}. These values were extracted from the full distributions of the collected sediment samples. Aeolis can simulate multi-fraction sediment transport incorporating sorting and armoring processes using a full grain size distribution (Hoonhout and de Vries, 2016). However, we used a three-fraction, cross-shore uniform bed layer for faster computational processing. In Experiment 1, we used the sediment grain size distributions (D_{10}, D_{50}, and D_{90}) measured from the SCB5, SHB8, SCB1, and NCB17 field sites (Runs 1.1, 1.8-1.10). For Experiment 2, we used sediment grain sizes D_{10} and D_{90} measured at the SCB5 site and only varied the median grain size (D_{50}) in the model.

The CDM model core of Windsurf computes spatially varying bed shear stress due to the presence of vegetation above a specified elevation and includes a linear growth rate for the fraction of vegetation cover. Within Windsurf, the vegetation limit is fixed at a vertical contour (minimum vegetation elevation) rather than at a fixed cross-shore location so as to allow for horizontal migration of the dune that could change the beach width (Cohn et al., 2019a). In this study, we explored the effect of minimum vegetation elevation in our model runs. Although other vegetation characteristics such as growth rate, plant density, and aboveground and belowground biomass have been shown to influence dune morphology (Biel et al., 2019; Bryant et al., 2019; Charbonneau et al., 2021; Feagin et al., 2015; Hacker et al., 2019; Hesp, 1989; Hesp et al., 2019; Jay et al., 2022; Zarnetske et al., 2015, 2012), exploration of these parameters in the model or the data sets was beyond the scope of this study.

3. Results

3.1. Observed Variability in Interannual Rates and Characteristics of Dune Evolution

Field measurements of cross-shore profiles at four representative field sites, SCB5, SHB8, SCB1, and NCB17, show highly variable dune evolution from 2016-2019, and illustrate the variation in rates and characteristics of change observed within CALO (Figure 1; Figure 2). For example, from 2016-2017, the foredune at SCB5 accreted vertically but then was overtopped and lost significant volume by 2018. It then began to show recovery by 2019, with foredune building occurring approximately 20 meters landward of the initial dune crest position. In contrast, the foredune at SHB8 remained relatively stable from 2016-2019. Erosion occurred on the beach and at the dune toe, resulting in a vertical scarp at the base of the dune. Likewise, the foredune at SCB1 had minimal vertical dune growth, but dune volume increased due to horizontal growth on both the seaward and landward sides of the dune crest. Finally, the foredune at NCB17, which was in an area that was overwashed prior to 2016, grew rapidly on its seaward side. At these four sites, dune volume change ranged interannually from 0.9 to 10.6 m^3/m in 2016-2017, -21.0 to 13.1 m^3/m in 2017-2018, and 0.0 to 5.4 m^3/m in 2018-2019.

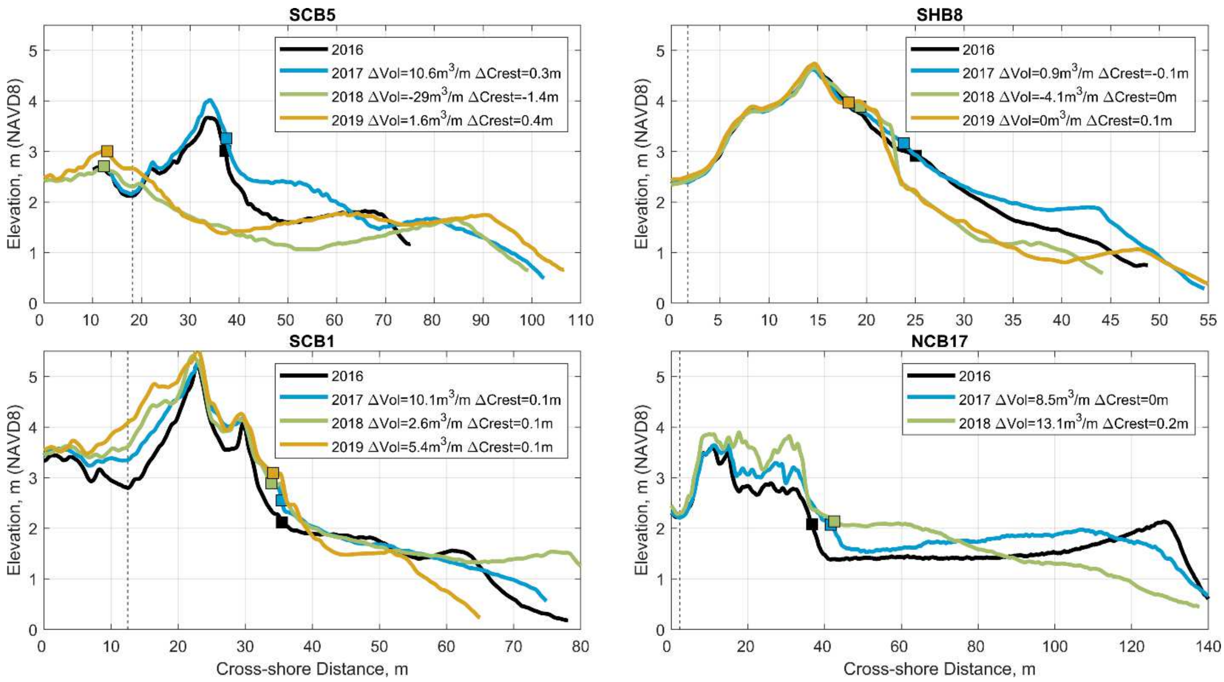

Figure 2. Observed variation in rates and characteristics of dune evolution at four field sites: SCB5, SHB8, SCB1, and NCB17 (Figure 1). Changes in the dune volume (∆Vol) and crest elevation (∆Crest) are computed interannually. The vertical, black dotted line represents the 2016 dune heel and landward-most extent used to calculate dune volume change. The squares show the measured minimum vegetation elevation and its cross-shore location on the profile for each year. NCB17 was not surveyed in 2019 due to unsafe field conditions caused by Hurricane Dorian.

Dune volume changes computed for all 55 field transects in CALO showed spatially and temporally varying response from 2016-2019 (Figure 1). Dune volumes increased by an average of 2.9 (standard deviation, σ=5.4) from 2016-2017 and by 1.6 (σ=9.1) m^3/m from 2018-2019 (Figure 1). Widespread erosion occurred across all islands from 2017-2018 (mean, μ=-11.9 m^3/m), with some sites eroding by as much as 20 m^3/m. This significant erosion is attributed to Hurricane Florence, which passed south of CALO in mid-September of 2018, approximately one month prior to our field data collection (NOAA, 2018). The period from 2017-2018 also resulted in the greatest variability in dune volume change (σ=12.8 m^3/m). Despite the widespread erosion that occurred within much of CALO during this period, the northern-most region of NCB increased in volume.

During the study period, changes occurred at the dune toe cross-shore location and the dune toe and crest elevation. Changes in these metrics were plotted against each other (Figure 3) to show the varying characteristics of dune change that occurred. We classified dune change in terms of horizontal progradation (Quadrants (Q) I and IV) and retreat (QII and QIII) and vertical accretion (QI and QII) and erosion (QIII and QIV) (Figure 3). Profiles within Quadrant IV exhibited an inverse relationship between dune toe elevation and cross-shore location, where dune toe progradation coincided with erosion (Figure 3a). The majority of dune toe retreat and erosion occurred from 2017-2018 (Figure 3a, QIII). In contrast, many profiles prograded and accreted at the dune toe from 2016-2017 (Figure 3a, QI). The relationship between dune toe location and dune crest elevation change was also variable (Figure 3b). Dune crest accretion occurred at profiles that experienced progradation and retreat at the dune toe (Figure 3b, QI and II). However, dune crest erosion combined with toe retreat were the most prevalent characteristic of dune evolution from 2017-2018 (Figure 3b, QIII). Note that incipient dune formation did not occur at any of the field sites between 2016-2019.

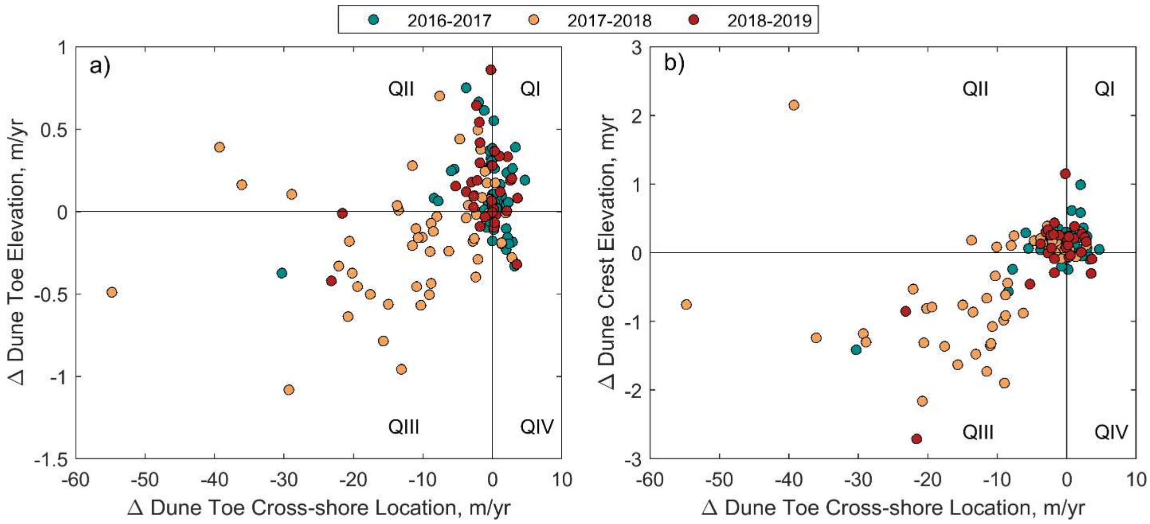

Figure 3. Relationship between the interannual change (2016-2017, 2017-2018, and 2018-2019; represented by the different colors) in dune toe cross-shore location and (a) dune toe elevation and (b) dune crest elevation. Quadrants (QI-IV) represent different characteristics of dune change (i.e., progradation and retreat of the dune toe cross-shore location and erosion and accretion of the dune toe and crest elevation).

3.2. Variability in Foredune Growth Factors

3.2.1. Pre-existing Morphology

Cross-shore topographic profiles at the SCB5, SHB8, SCB1, and NCB17 field sites in 2016 showed differing pre-existing morphologies (Figure 2; Figure 4). The dune at SCB1 was the tallest (5.2 m) followed by SHB8 (4.7 m). The crest heights on SCB5 and NCB17 were both approximately 3.6 m. Dune toe elevations were also lower at SCB5 and NCB17 compared to SCB1 and SHB8. SHB8 had the steepest foreshore beach and dune face slopes, narrowest beach width, and largest dune volume of all four profiles. The dune at NCB17 was fronted by the widest, shallowest beach. At the MSL contour (-0.11 m), the beach was shallowest at NCB17 (0.021 m/m), and steepest at

SCB5 (0.063 m/m) (Figure 4). At the -6 m contour, the shoreface was shallowest at SCB1 (0.004 m/m) and steepest at NCB17 (0.035 m/m).

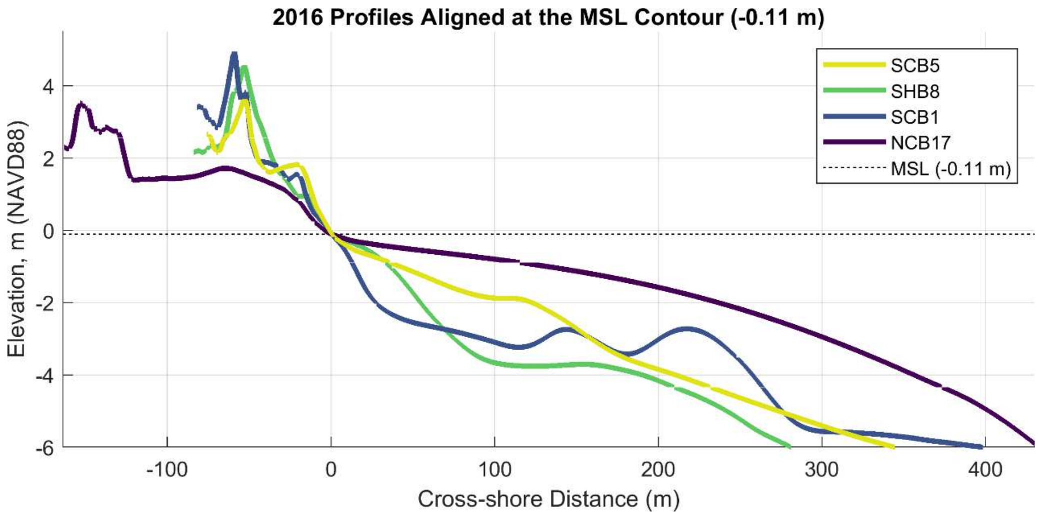

Figure 4. Observed 2016 beach and dune topography at SCB5, SHB8, SCB1, and NCB17 sites (Figure 1), merged with bathymetry from the National Centers for Environmental Information (NCEI) digital elevation model (DEM). Profiles have been aligned at the mean sea level (MSL) contour (-0.11 m) to emphasize morphological differences.

3.2.2. Environmental Forcing Conditions

Wave hindcasts from the offshore WIS station nearest to each of the four field sites (63272 for SCB5, 63287 for SHB8 and SCB1, and 63268 for NCB17) revealed that the October 2016-2017 dominant wave direction was from the southeast (mean of all three WIS stations, μ=141.8˚ and σ=61.3˚. Wave direction is reported in degrees relative to a nautical convention, e.g., the direction waves come from, measured clockwise from geographic North). The average wave height was 1.3 m (σ=0.6 m) and the average peak wave period was 7.5 sec (σ=2.3 sec). The last two months of the environmental timeseries (i.e., 08-09/15/17 and 09-10/15/2017) showed increased wave heights and longer wave periods (Figure 5b,d), which are attributed to multiple storms that passed within a 500 km radius of CALO during this period including an unnamed tropical storm (Aug.27-29), Hurricane Gert (Aug. 12-18), Hurricane Jose (Sept. 4-25), and Hurricane Maria (Sept.16-Oct. 2) (NOAA, 2018). The dominant wind direction, observed at the NOAA CLKN7 weather station from 2016-2017, was from the northeast and southwest and the average windspeed was 5.6 m/s (σ=2.7 m/s). The 2016-2017 wave and wind characteristics did not differ substantially from multi-decadal trends (not shown). The multi-decadal (1980-2019) dominant wave direction was also from the southeast (μ=132.1˚ and σ=52.6˚), and the multi-decadal average wave height and period were 1.2 m (σ=0.6 m) and 8.4 sec (σ=2.4 sec), respectively. The multi-decadal (1997-2019) dominant wind direction was also from the northeast and southwest and the average windspeed was 5.7 m/s (σ=2.9 m/s).

Within the entirety of CALO, the shore-normal angle ranged from 101-255˚ (Table 4). At the SCB5, SHB8, SCB1, and NCB17 field sites, the shore-normal angle ranged from 115-207˚ (Table 4). The offshore WIS station nearest to each of the four field sites showed the wave height and period varied minimally among the WIS stations from October 2016 to 2017 (Table 1; Figure 1; Figure 5b,d); the most significant difference was the onshore wave direction (Figure 5c). Note that in Figure 5c, the wave directions experienced at all four sites have been oriented to use 0˚ as the onshore wave direction, rather than the site-specific shore-normal angle, to allow better comparison of onshore directed waves among the four sites. SCB5 and NCB17 were more exposed to onshore directed waves, with 87% and 91% of waves, respectively, directed within ± 90˚ of shore-normal. In contrast, only 67% (SHB8) and 39% (SCB1) of the hourly wave conditions were oriented onshore for the other two sites. However, the average wave height of onshore directed waves (1.2-1.3 m) did not vary significantly among the four field sites. The cross-shore component of the wind velocity, calculated from the NOAA CLKN7 weather station, varied with time and field site due to the varying shoreline orientation (Figure 5e). The average cross-shore wind velocity was larger at SHB8 (4.0 m/s) and SCB1 (3.6 m/s) and smaller at SCB5 and NCB17 (2.4 m/s at both).

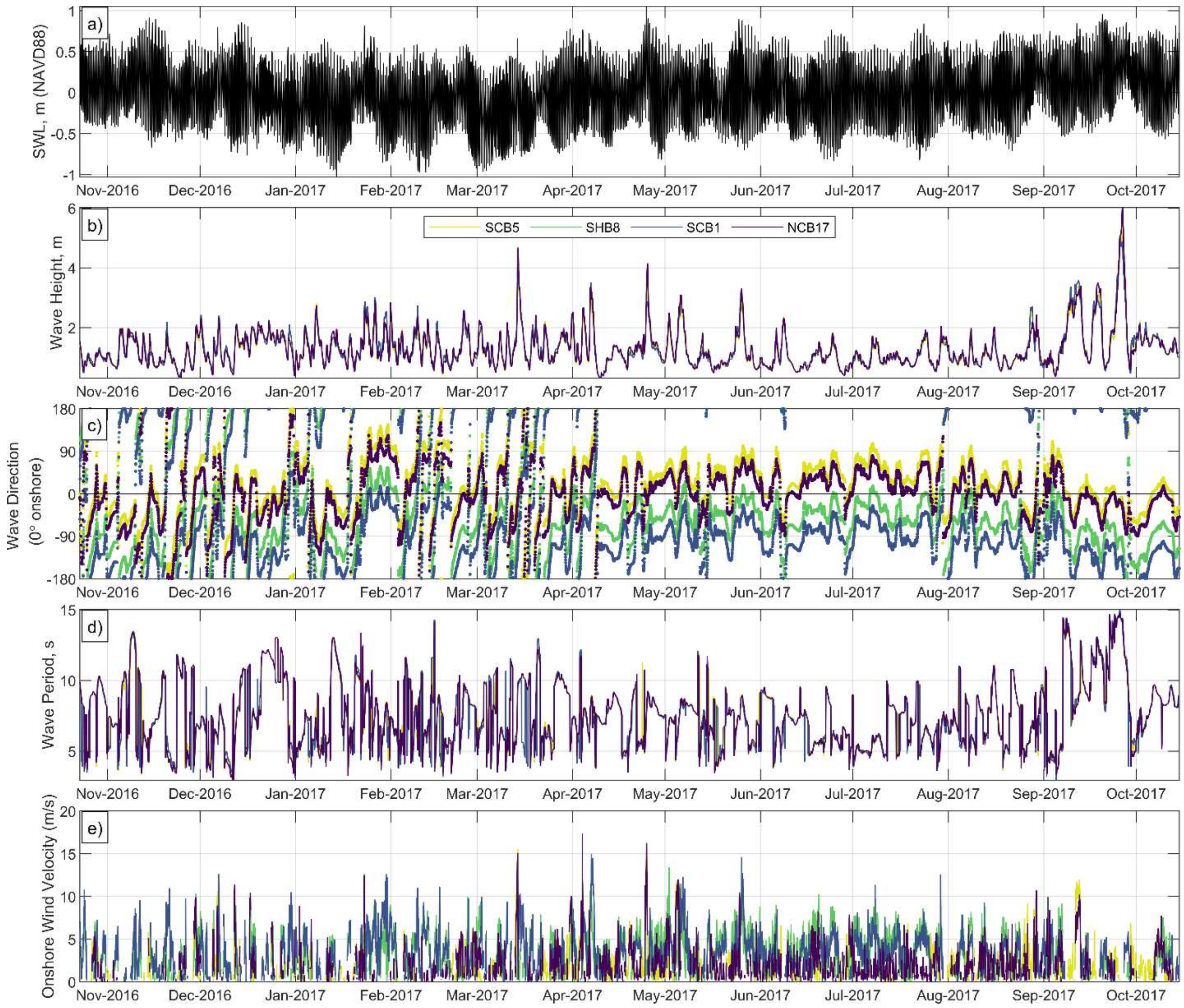

Figure 5. Time series of environmental forcing variables from October 2016-2017. (a) Still water level (SWL) from NOAA tide gauge 8656483, (b) wave height, (c) wave direction, and (d) wave period from USACE WIS stations (63272, 63287, and 63268), and (e) onshore wind velocities from NOAA weather station CLKN7. The colors represent wave and wind data from the WIS stations located nearest the field sites: SCB5 (63272), SHB8 (63287), SCB1 (63287), and NCB17 (63268) (Figure 1). The onshore wave and wind data at each field site are shown. The onshore wave direction relative to each field site is represented by 0˚ in panel c.

3.2.3. Sediment Grain Size Distribution

Within CALO, the median sediment grain size varied from 0.14-0.44 mm (Figure 6). Larger grain sizes were observed along the east-west oriented shorelines of SHB and southernmost region of SCB. Sediment sorting values tended to vary with median grain size; poorer sediment sorting occurred at sites with larger median grain sizes. At the SCB1, SCB5, NCB17 and SHB8 field sites, the median sediment grain sizes ranged from 0.24-0.43 mm, and classified as moderately to moderately well sorted (Table 3, Figure 6) (Folk, 1968; Folk and Ward, 1957; Pettijohn et al., 1987). SCB5 and NCB17 had similar median sediment grain sizes (0.25 and 0.24 mm, respectively) and sorting values (0.5 phi; moderately well sorted). SCB1 had the coarsest median grain size (0.43 mm) and the most poorly sorted distribution (0.9 phi; largest sorting value).

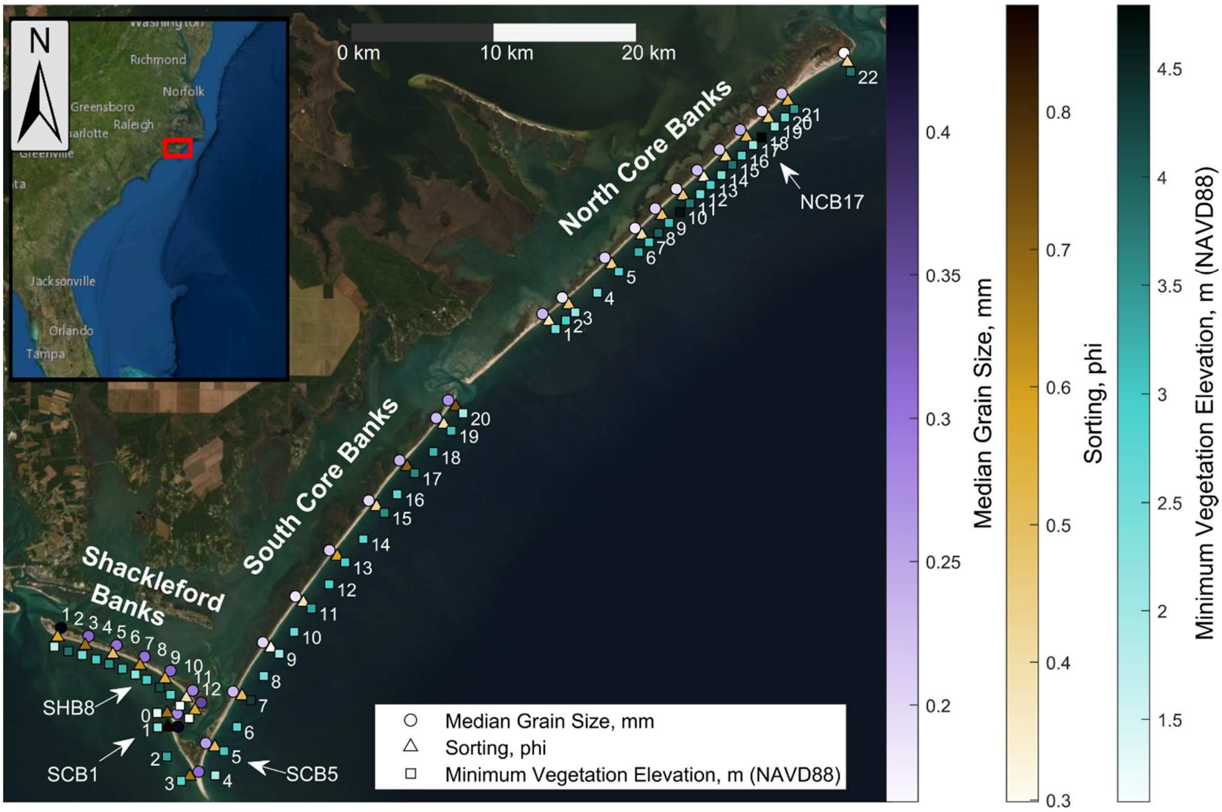

Figure 6. Sediment grain size and minimum vegetation elevation at all 55 field sites in the Cape Lookout National Seashore, NC study region. Median grain size (D_{50}, mm; represented by the circles) and sorting (phi; represented by the triangles) are from 2016 (SCB1 and SCB5) and 2017 (all other sites). The minimum vegetation elevations (squares) are from 2016. Marker colors indicate the values of the sediment grain size and minimum vegetation elevation. The top left inset shows the location of CALO relative to the U.S. Atlantic coast.

3.2.4. Minimum Vegetation Elevation

The average minimum vegetation elevation from 2016-2019 along all CALO field sites was 3.1 m (σ=0.9 m) and ranged from 0.9 m to 6.6 m (Table 4). The average minimum vegetation elevation in 2016 was 2.9 m (σ=0.8 m) and ranged from 1.1 m to

4.8 m (Figure 6). The minimum vegetation elevation gradually increased at more northernly latitudes and was, on average, higher on NCB than on SCB and SHB (Figure 6). At the SCB5, SHB8, SCB1, and NCB17 field sites, the minimum vegetation elevation was 3.0 m, 2.9 m, 2.1 m, and 2.1 m, respectively (Table 3; Figure 6). For additional information on vegetation measurements including distribution, abundance, and density of dune grass species in CALO refer to Hacker et al. (2019) and Jay et al. (2022).

3.3. Windsurf Model Calibration

Windsurf was calibrated for one year (October 2016-2017) using SCB5 observations for the model parameters Cb, facSk, and facAs (Table 2). The observed profiles from 2016 and 2017 showed sediment deposition on the beach, resulting in increased bed elevation and shoreline progradation (Figure 7). During this time, the dune volume increased by 10.9 m^3/m and the dune crest elevation increased by 0.3 m. The calibrated Windsurf model generally captured these observed changes, but slightly underestimated the dune volume change by 0.32 m^3/m and dune crest change by 0.05 m (Table 2; Figure 7). The modeled profile has a RMSE of 0.12 m and Brier Skill Score of 0.96 (Table 2).

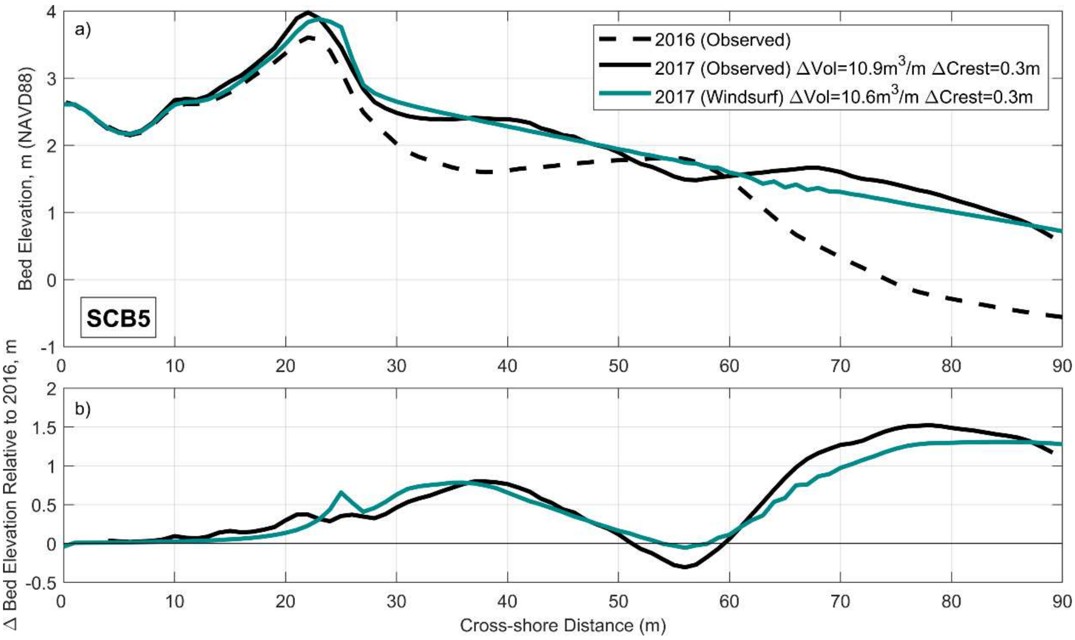

Figure 7. The coastal profiles at the SCB5 field site between 2016 and 2017 using a) observed (black) and Windsurf-calibrated (teal) bed elevations, and b) their change. Change in the dune volume (ΔVol) and crest elevation (ΔCrest) reported in the legend were computed between the 2016 (observed) and 2017 (observed and calibrated) profiles.

3.4. Model Response to Variations in Factors Influencing Dune Growth

3.4.1. Experiment 1 Model Runs

The Experiment 1 modeling suite (Table 3) was run using the calibrated model parameters and the observed pre-existing morphology, environmental forcing conditions, sediment grain size, and minimum vegetation elevation at SCB5 (Run 1.1 baseline model). The values for each factor were then changed in the model one at a time to represent observed conditions at the SHB8, SCB1, and NCB17 field sites. All other values in Windsurf were held constant across all of the simulations (Runs 1.2-1.13).

The simulations testing the influence of varying pre-existing nearshore, beach, and dune morphology (Runs 1.1, 1.2-1.4) resulted in dunes that evolve at different rates and exhibit different types of growth (Figure 8a). Run 1.3, which used the SCB1 pre-existing morphology, had the tallest initial dune crest and accreted at the dune crest by 0.5 m, more than any other profile. Run 1.4 (NCB17 pre-existing morphology) developed an incipient dune seaward of the existing foredune at the 20 m cross-shore location, which resulted in vertical growth of 1.1 m. Run 1.1 (SCB5 pre-existing morphology, baseline simulation) had the most sediment deposition above the 2 m contour. Run 1.2 (SHB8 pre-existing morphology), which had the steepest foreshore beach slope and narrowest beach width of the four initial profiles, experienced the least amount of sediment deposition above the 2 m contour and at the dune crest.

The simulations testing the environmental forcing conditions were varied according to the shoreline orientation at each of the four field sites. Runs 1.1 and 1.7 used environmental conditions from SCB5 and NCB17, respectively, which are located on east facing shorelines that are more exposed to the dominant wave direction (Figure 1; Figure 5). These model runs showed substantial sediment accumulation above the 2 m contour (Figure 8b). The bed elevation at the 30 m cross-shore location increased by 0.6 m for both model runs. Runs 1.5 and 1.6 used SHB8 and SCB1 environmental conditions, respectively. These sites are more sheltered from wave action but are exposed to the dominant cross-shore wind direction (Figure 5). In these model simulations, sediment moved higher onto the beach (around 37 m in the cross-shore) compared to the results of simulations testing the influence of pre-existing morphology. The dune crest accreted 0.3 m for Runs 1.1 and 1.6 (SCB5 and SCB1 environmental conditions, respectively) and 0.2 m for Runs 1.5 and 1.7 (SHB8 and NCB17 environmental conditions, respectively).

Variations in modeled beach and dune change due to variability in sediment grain size were slight, especially relative to the influence of variability in the initial morphology and environmental conditions (Figure 8c). The coarsest and most poorly sorted sediment (Run 1.9; SCB1 sediment) produced the least dune crest growth. Finer sediment (Run 1.1; SCB5 sediment and Run 1.10; NCB17 sediment) resulted in the most accretion at the crest (0.3 m of vertical change for both simulations) and on the seaward and landward side of the crest (not apparent at the scale shown in Figure 8c, however the measured change between the 2016 observed and 2016-2017 modeled Windsurf profile elevations at the cross-shore distance x=25 m and x=20 was 0.3 m and 0.1 m, respectively, for both Run 1.1 and Run 1.10). This resulted in a wider dune near the crest and steeper dune face slope. Sediment from SHB8 (Run 1.11), which was coarser than SCB5 (Run 1.1) and NCB17 (Run 1.10) but finer than SCB1 (Run 1.9), resulted in relatively intermediate crest accretion and increased dune volume.

Simulations with lower minimum vegetation elevations (i.e., Run 1.12; SCB1 and Run 1.13; NCB17) resulted in increased sediment accretion in front of the dune, particularly near the 2.1 m contour where vegetation was present, thereby stunting vertical dune growth landward of this contour (Figure 8d). Dunes with higher minimum vegetation elevations (i.e., Run 1.1; SCB5 and Run 1.11; SHB8) developed taller dunes that were wider near the crest.

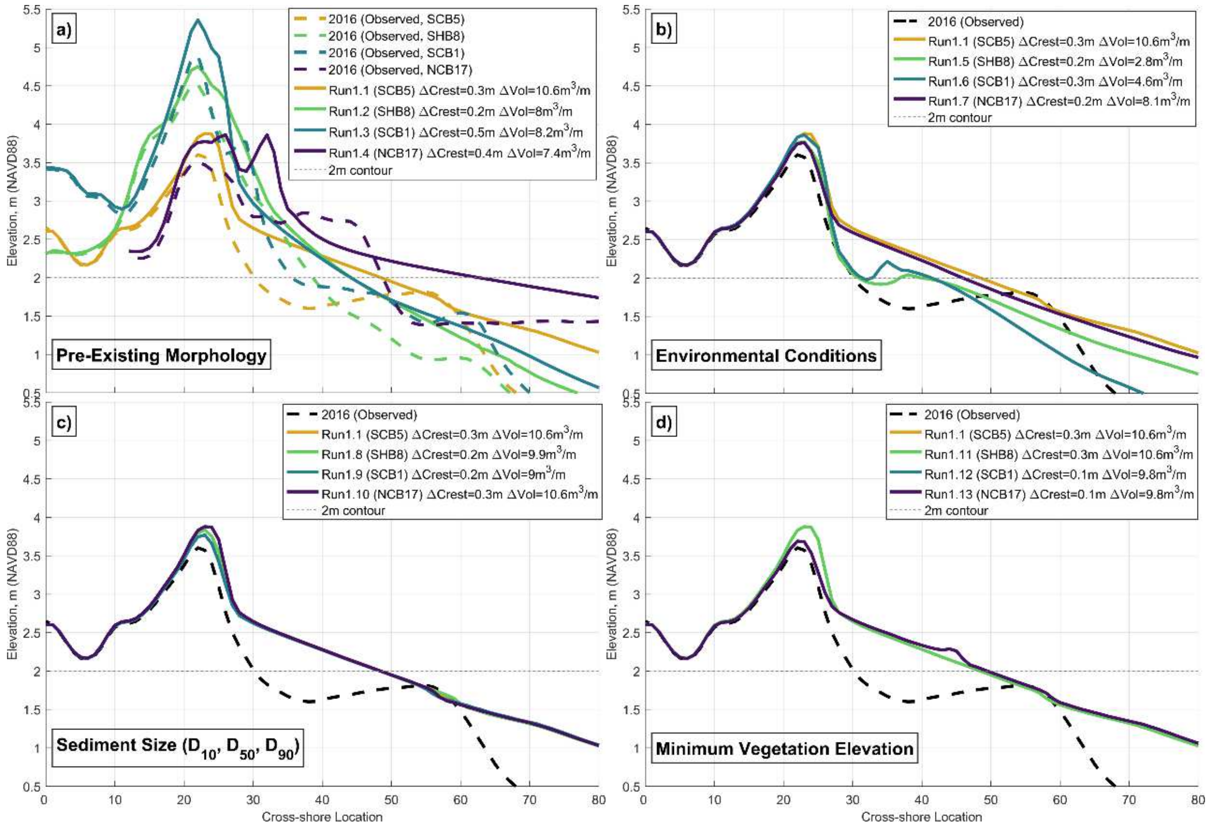

Figure 8. Profiles for the observed elevations in 2016 and the Windsurf modeled profiles (2016-2017) for each run in Experiment 1 using the varying a) pre-existing morphology, b) environmental forcing conditions, c) sediment grain size (D_{10}, D_{50}, D_{90}), and d) minimum vegetation elevation derived from in-situ values at the SCB5, SHB8, SCB1, and NCB17 field sites (Table 3).

Modeled changes in the dune crest elevation and dune volume for each model run in Experiment 1 (Table 3) are shown in Figure 9. The dune crest elevation change varied most, within a range of 0.23 m, for simulations with varying pre-existing morphologies (Runs 1.1-1.4; Figure 9). The range of dune volume change was most influenced by changes in the environmental boundary conditions and varied by 7.8

m/m^3 in Runs 1.1, 1.5-1.7. Minimum vegetation elevation had a larger effect on dune crest elevation than sediment grain size, but varying sediment grain size resulted in more dune volume change. Changes in the dune crest elevation and dune volume were often synchronized among the varying boundary conditions, meaning that increases in the crest relative to the baseline scenario coincided with increases in dune volume and vice versa. Runs 1.3 and 1.4, which used the pre-existing morphology from SCB1 and NCB17, respectively, were exceptions to this pattern. For these model runs, the dune crest elevations increased relative to the baseline scenario and the dune volumes decreased.

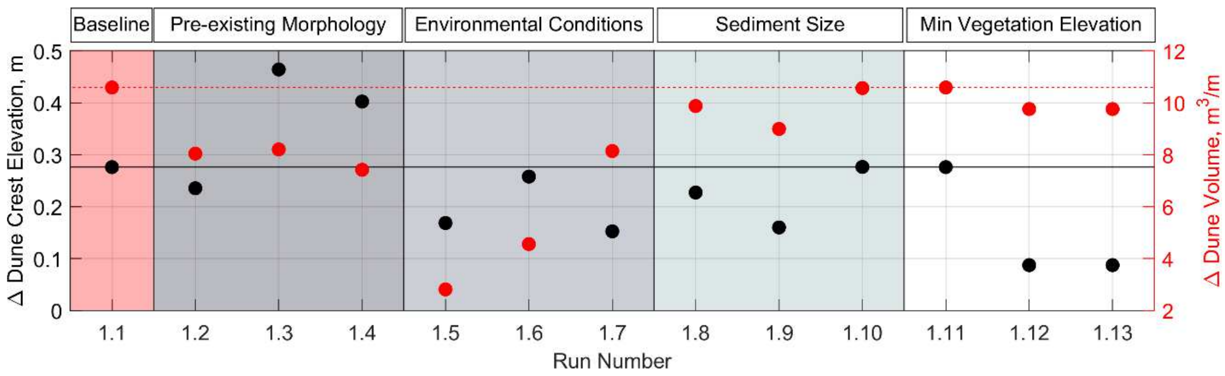

Figure 9. Change in dune crest elevation (left axis; black) and dune volume (right axis; red) from Experiment 1 model runs using varying pre-existing morphology, environmental forcing conditions, median sediment grain size, and minimum vegetation elevation at the SCB5, SHB8, SCB1, and NCB17 field sites (Table 3). The horizontal lines represent the baseline (Run 1.1; the calibrated model at SCB5) changes in the dune crest and volume.

3.4.2. Experiment 2 Model Runs

The Experiment 2 modeling suite (Table 4) involved 19 simulations using the full range of observed foredune growth factors within CALO (2016-2017), including the environmental forcing conditions dictated by the shore-normal angle, median sediment grain size, and minimum vegetation elevation. Calibrated and all other model parameters were held constant among the model runs.

Of the factors tested in the Experiment 2 modeling suite, the environmental forcing conditions dictated by the shore-normal angle produced the most variable change in dune crest elevation and dune volume (Figure 10a,d). For shore-normal angles between 100-130˚ (Runs 2.1-2.6), change in both the dune crest elevation and dune volume decreased. The minimum change in these metrics occurred at 160˚ (Run 2.3) and then increased at progressively larger shore-normal angles (Runs 2.4-2.6). Somewhat surprisingly, dune volume increase was greater for coastlines exposed to the southeast (i.e., the dominant wave direction) as opposed to the southwest (i.e., the dominant wind direction).

Model runs varying the median grain size (Runs 2.7-2.13) revealed that as sediment grain size increased, dune crest elevation change and dune volume change both decreased (Figure 10b,e). Likewise, as minimum vegetation elevation increased, change in the dune crest elevation and dune volume increased (Figure 10c,f). At elevations of 2.5 m and higher (Runs 2.17-2.19), the effect of the minimum vegetation elevation on the coastal profile plateaued, and there was minimal change to the response variables; change in the dune crest elevation and dune volume stabilized at 0.28 m and 10.6 m^3/m, respectively. Comparing modeled results between the varying median sediment grain size and minimum vegetation elevation factors (Runs 2.7-2.19), the finest median sediment grain size (0.15 mm; Run 2.7) resulted in the greatest positive change in dune crest elevation (0.31 m) and dune volume (11.2 m^3/m). The lowest minimum vegetation elevation (1.0 m; Run 2.14) resulted in no dune crest elevation change (0 m) and the lowest change in dune volume (6.5 m^3/m).

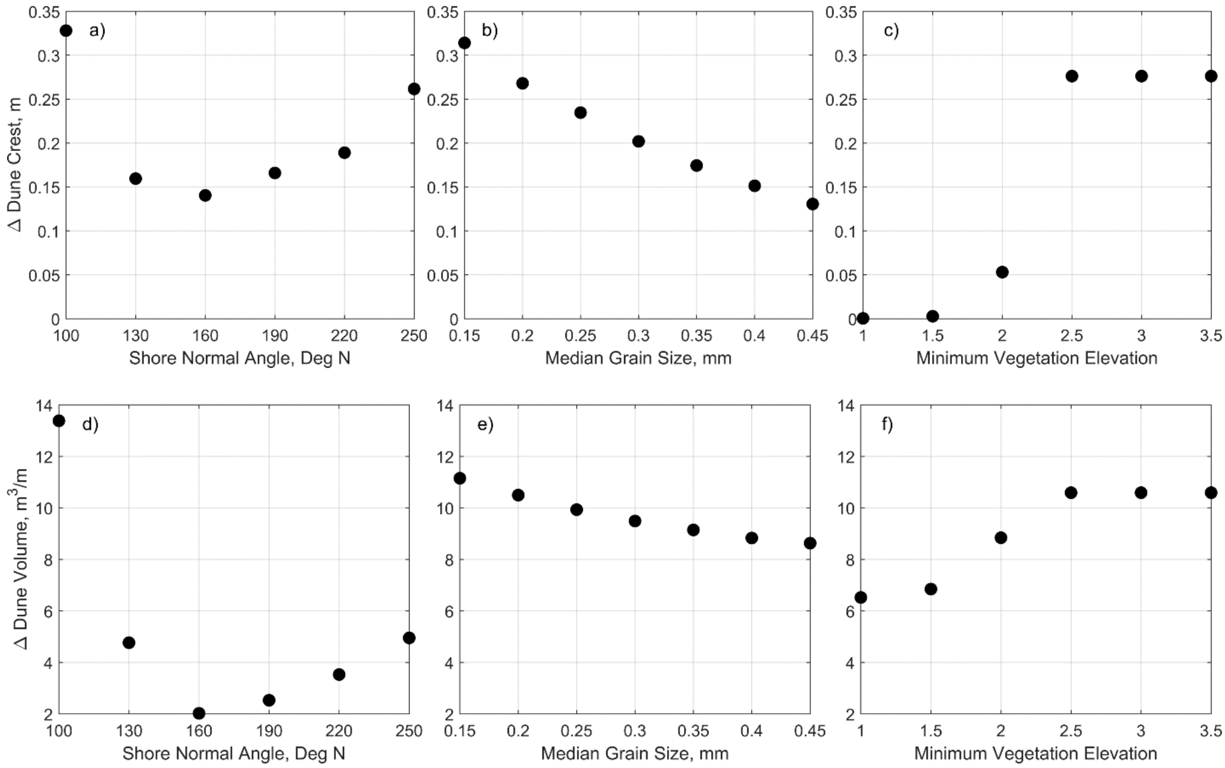

Figure 10. Change in the dune crest elevation (a-c; top row) and dune volume (d-f; bottom row) from Experiment 2 using varying shore-normal angles that influence environmental forcing conditions, median sediment grain sizes, and minimum vegetation elevations (Table 4).

To further explore the marine and aeolian processes driving different beach and dune responses for the varying shore-normal angles shown in Figure 10a,d, the change in bed elevation associated with each of these processes is presented at the monthly timescale (Figure 11). Marine- and aeolian-driven bed changes are defined as those modeled in Windsurf's model cores, XBeach (marine) and Aeolis (aeolian). The total monthly bed elevation change was influenced more by marine processes than by aeolian processes at smaller shore-normal angles (e.g., 100˚ and 130˚), which were more exposed to the dominant southeast wave direction (i.e., μ=141.8˚). Compared to other shore-normal angles, 100˚ and 130˚ had larger marine-driven bed elevation change rates which occurred at locations along the beach to the base of the dune (near the 30 m cross-shore location). For the 100˚ and 130˚ shore-normal angles, the dune crest (near the 20 m cross-shore location) accreted more as a result of aeolian-driven transport. As shore-normal angles increased from 160˚ to 250˚, and thus became more sheltered from waves coming from the dominant direction and more exposed to the southwest cross-shore wind direction, the monthly bed elevation change became more influenced by aeolian processes. Interestingly, for these shore-normal angles (e.g., 160˚ to 250˚), the majority of the onshore migration of the pre-existing beach berm feature (initially near the 55 m cross-shore location) resulted from aeolian transport rather than marine transport (Figure 11). The shore-normal angle of 160˚, which experienced the least amount of change in dune crest elevation and dune volume (Figure 10a,d), was oriented in neither the dominant wind nor wave direction. At this shore-normal angle, both monthly marine and aeolian bed elevation changes were relatively smaller (Figure 11).

The change in monthly bed elevation also varied with time (Figure 11). For shore-normal angles of 100˚ and 130˚, a large amount of sediment was deposited on the beach in the last two months of the simulation (i.e., 08-09/15/17 and 09-

10/15/2017). For sites with shorelines that were more sheltered from the dominant wave action (i.e., 190-250˚), there was no marine-driven bed elevation changes during this time and aeolian-driven sediment transport was minimal. The largest monthly bed elevation changes associated with aeolian sediment transport occurred during the months of March to July.

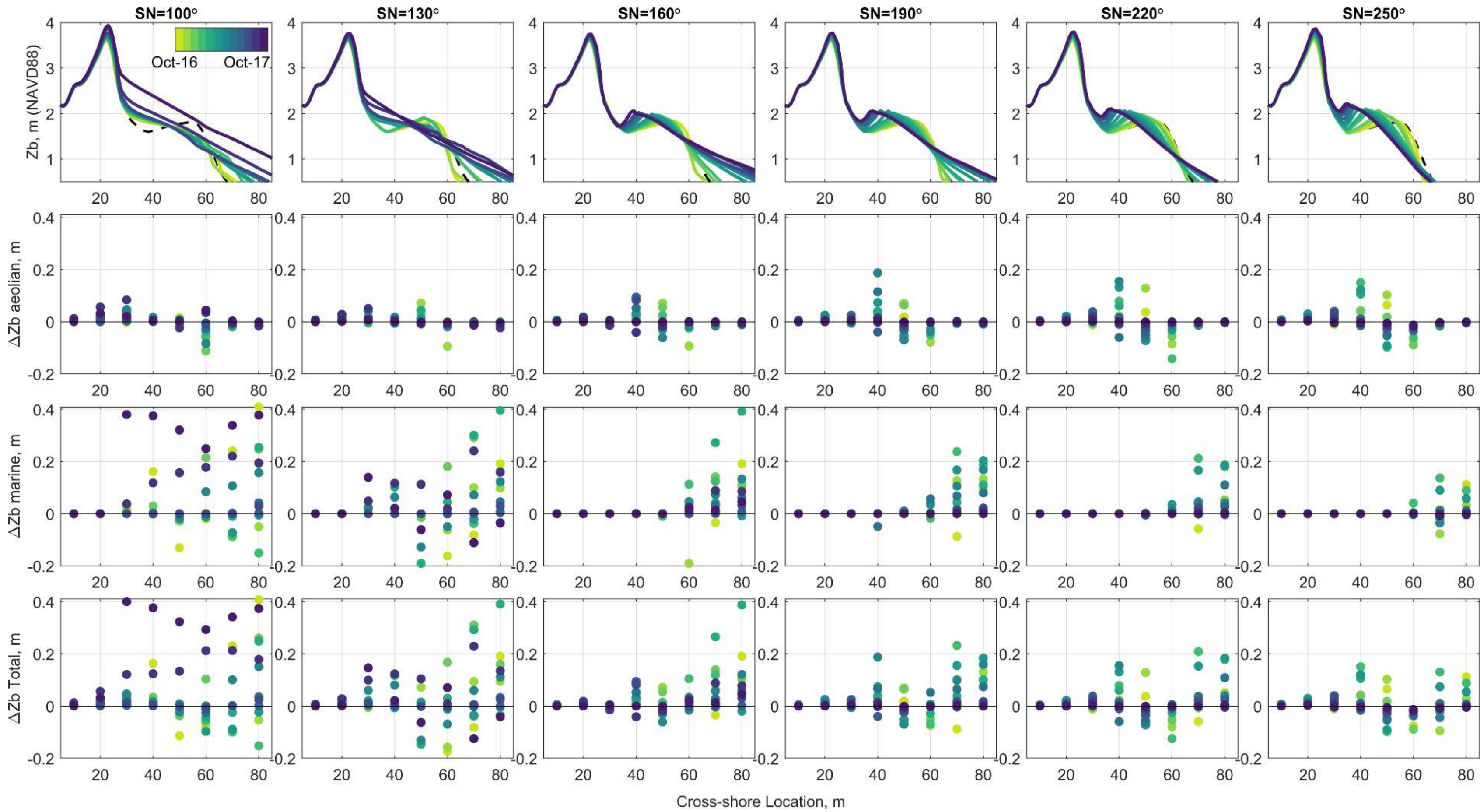

Figure 11. Profiles of the monthly bed elevation (Zb; first row) and changes in aeolian-driven bed elevation (ΔZb aeolian; second row), marine-driven bed elevation (ΔZb marine; third row), and total bed elevation (ΔZb total, aeolian- plus marine-driven; fourth row) for each shore-normal (SN) angle from Experiment 2, Runs 2.1-2.6 (Table 4; columns). The bed

elevation changes are shown at discrete cross-shore locations across the profile (x-axis), and the colors represent the monthly timescale from October 2016-2017. The black dashed line beneath the colors in the figures in the top row (most visible in the top left plot) represents the initial profile.

4. Discussion

4.1. Relative Influence of Foredune Growth Factors

Of the four factors influencing foredune growth explored in this study, findings from the suite of simulations in Experiment 1 indicate that the pre-existing morphology of the beach and dune has the largest influence on subsequent dune evolution (Figure 8). The model results show that the pre-existing morphology alters the rates and types of dune growth, especially the range of dune crest growth and the formation of incipient dunes (e.g., Run 1.4). The pre-existing morphology is likely the most influential factor of foredune change explored in this study because it encompasses many variables (e.g., foreshore beach slope, shoreface slope, and beach width) that have been shown to affect subaqueous and subaerial sediment transport, and thus dune change during storms and recovery (Crapoulet et al., 2017; Héquette et al., 2019; Hesp and Smyth, 2016; Larson et al., 2004; Ruggiero et al., 2001; Sherman and Bauer, 1993; Short and Hesp, 1982). For example, dune growth is smallest for the model simulation that used the SHB8 morphology (Run 1.2); this is attributed to limited sediment transport rates to the dune, caused by the narrow, steep beach at this site and thus larger runup and restricted fetch length. The wider, shallower sloped beaches for the SCB5 (Run 1.1), SCB1 (Run 1.3), and NCB17 (Run 1.4) morphologies result in lower runup, longer fetch lengths, higher transport rates to the dune, and thus more dune growth.

The model simulations show that the rate of foredune growth, particularly the range of dune volume change, is most influenced by the environmental forcing conditions (Figure 8; Figure 10). We found that dune volume increases on shorelines that are exposed to either the dominant wave direction or the dominant wind direction, with larger change occurring for the former (Figure 11). The significant amount of marine-driven beach deposition that occurred on east facing shorelines during the last two months of the simulations (Figure 11) coincide with increased wave heights and longer periods relative to the average 2016-2017 wave conditions (Figure 5). This is attributed to multiple storms during this period including an unnamed tropical storm and Hurricanes Gert, Jose, and Maria. These conditions resulted in taller dunes due to increased sediment supplied by marine processes that was subsequently transported to the dune crest via aeolian-driven transport. These conditions also resulted in dunes on east facing shorelines that were greater in volume due directly to marine-driven sediment transport to the base of the dune (above the 2 m contour) compared to the south- southwest-facing shorelines that were more sheltered from wave action during the period of study. These findings suggest that for certain hydrodynamic conditions (i.e., elevated water levels, larger waves, and longer periods) and shoreline orientations, marine processes may be a significant contributor to rapid and substantial foredune growth. These model results are consistent with recent field data (Cohn et al., 2018) and numerical modeling simulations (Cohn et al., 2019a) for dissipative beaches, which have shown specific marine processes (i.e., infragravity swash, high still water levels, and/or energetic wave conditions) can drive approximately 9%-38% of annual dune growth. Similarly, these results are consistent with the positive, long-term relationship found between foredune height and wave height (Durán and Moore, 2013; Hesp, 1988; Miot da Silva et al., 2008; Moulton et al., 2021; Pellón et al., 2020; Ruggiero et al., 2005; Short and Hesp, 1982).

Even though the hydrodynamic conditions during this study resulted in beach and dune growth on exposed shorelines, more elevated water levels and energetic wave conditions than those observed in our study period (such as those produced during hurricanes and nor'easters) have the potential to erode and overtop dunes within this region (Dolan and Lins, 1985; Hovenga et al., 2021; Passeri et al., 2020; Riggs and Ames, 2007; Stockdon and Thompson, 2007). Our findings suggest that the future resiliency of dune-backed coastlines in CALO will be affected by projected changes in storminess patterns, shifts in the wave climate, and sea-level rise (Hicke et al., 2022; Wang et al., 2004; Woolf et al., 2002). More research is needed to explore the magnitude and frequency thresholds (Pellón et al., 2020) of marine-driven construction and erosion of coastal dunes for present-day and projected future conditions.

Our model simulations show that dune crest elevation and dune volume both increase as the median sediment grain size decreases; however, sediment grain size is less influential in altering these foredune metrics compared to the other factors explored in this study (Figure 9; Figure 10). For example, within CALO the range of observed sediment grain sizes (0.17 mm to 0.44 mm) resulted in less dune crest elevation and volumetric change than variations in both the minimum vegetation elevation and the shore-normal angle, suggesting that sediment grain size is less influential in altering foredune rate and type of growth in this region (Figure 10). However, the finest sediment size investigated (0.15 mm) produced taller dunes and larger dune volumes when compared to any of the observed minimum vegetation elevations within CALO. This result suggests that the presence of very fine sediments could be an important factor contributing to dune morphology.

The model simulations indicate that low minimum vegetation elevations can hinder dune crest growth and limit sand volume change above the two-meter contour (Figure 10). This is attributed to the reduced fetch length and increased drag of vegetation at lower elevations, which limit aeolian-driven transport and cause sediment to be deposited on the beach instead of in the dunes (Figure S1.1). For dunes that have higher minimum vegetation elevations, sediment is eroded from the beach and transported to the dune by aeolian-driven transport (Figure S1.1), resulting in more dune accretion. Modeled morphometric changes plateaued as the minimum vegetation elevation increased above 2.5 meters (Figure 10), indicating that the bed shear stress reduction is maximized for all minimum vegetation elevations near the dune crest (2.5 m and higher) and/or that, for these simulations, sediment availability or transport was limited. The minimum elevation at which vegetation establishes on the dune, and thus plant zonation, is related to the physiological tolerances of vegetation to sand burial and seawater inundation (Du and Hesp, 2020; Hacker et al., 2012; Levin et al., 2008; Maun, 2009; Mullins et al., 2019; Seneca, 1972). A correlation between plant zonation and beach type (dissipative vs. reflective) has been observed, in which increased foredune heights are linked to wider plant zonation on dissipative beaches as a result of decreased wave runup, salt spray, and sand salinity (Durán and Moore, 2013; Goldstein et al., 2017; Hesp, 1988; Miot da Silva and Hesp, 2010; Saye et al., 2005; Weng et al., 1991). For our simulations on an intermediate beach (Section S1.2), we found that lowering the minimum vegetation elevation and thus increasing the plant zonation reduced the beach width and thus the fetch length such that sediment availability and aeolian-driven transport was limited, ultimately resulting in shorter dunes that were wider near the base.

Although our findings are relevant at annual timescales, the relative importance of foredune growth factors investigated here (and others not explored in this study such as storm surge under sea-level rise, longshore transport gradients, armoring by sediment sorting, and variable beach grass density) may change according to timescale (seasonal to multi-decadal) (Carter, 1976; Carter and Rihan, 1978; Hoonhout and de Vries, 2016; McKenna Neuman et al., 2012; Passeri et al., 2018; Roelvink and Costas, 2019; Zarnetske et al., 2015). When considering management of coastal dunes, our findings suggest that management-based decisions which alter the pre-existing morphology, such as beach and dune grading and beach nourishment, may have considerable impacts on subsequent dune growth, particularly at annual timescales. Additionally, the grain size selected for beach nourishment projects could influence dune height and volume, such that the placement of sand that contains a greater proportion of coarser grains than naturally found on the beach could reduce dune growth. Finally, lowering the minimum vegetation elevation by planting further seaward than naturally would occur may limit vertical dune growth.

4.2. Model Parameterizations and Assumptions

The numerical model used in this study, and the factors of variable dune growth that were tested here, include different parametrization schemes and assumptions that could affect simulated dune growth. For example, the 1D cross-shore modeling approach that we used in this study does not incorporate the higher dimensional variability of bathymetric/topographic features (e.g., 2D sandbars, troughs, and cusps, and washover gaps in the dune line), all of which may influence dune evolution, particularly “hot spot” erosional effects (Castelle et al., 2019, 2017; Houser, 2013; Houser et al., 2008). Additionally, the variable environmental forcing conditions that we employed are developed for each site using a filtering process to orient wave and wind directions based on alongshore-averaged shoreline orientation. These wind and wave conditions are imposed as model boundary conditions, along with a still water level acquired from a single tide gauge. This approach simplifies or omits spatially varying storm surge and sea level anomalies, refractive effects, and dissipation, which may smooth or alter total water level variability along the shore (Serafin et al., 2019; Theuerkauf et al., 2014). More research incorporating alongshore varying total water levels developed via high fidelity hydrodynamic models is needed to understand the influence these processes may have on dune growth. Lastly, process-based beach-dune evolution models, including Windsurf, typically include adjustable coefficients that require calibration (Rafati et al., 2021). Additional testing is needed to explore the variability of these parameters in Windsurf (e.g., Cb, facSk, and facAs) among different field sites and determine the model’s aptness at capturing all possible foredune change (e.g., recovery and erosion) through time.

5. Conclusion

Annual field measurements in Cape Lookout National Seashore (CALO) showed temporal and spatial variability in foredune change including retreat / progradation and erosion / accretion. Model results using the coupled beach-dune evolution model Windsurf suggest that pre-existing morphology has the most significant influence on the type of foredune growth, which can vary from the development of incipient dunes to horizontal and/or vertical change of existing dunes. Environmental forcing conditions had the most influence on dune volume changes. Marine-driven sediment transport were shown to drive rapid and significant dune accretion and progradation. The full range of observed minimum vegetation elevations within CALO resulted in a larger deviation of dune crest elevation and volume change compared to the full range of observed median grain sizes.

Findings from this work may be used to inform coastal management decisions such as dune restoration, grass planting, beach and dune grading, and beach nourishment projects. By better understanding the ways in which important factors influence dune growth, coastal managers may prioritize which, where, and how different strategies are implemented. Within the scope of beach-dune modeling efforts, our findings can be used to inform physics, parameterization schemes, and incorporate management scenarios in numerical models (Itzkin et al., 2022; Ruggiero et al., 2019). Additionally, findings from this work improve our understanding of foredune growth and are significant to ongoing modeling efforts and field campaigns, coastal hazard predictions, and resiliency planning.

Acknowledgments

This work was funded by NOAA via the NOS/NCCOS/CRP Ecological Effects of Sea-Level Rise (EESLR) Program (grant no. NA15NOS4780172) to P.R., S.D.H., and L.J.M. and by the U.S. Coastal Research Program (USCRP) Cooperative Agreement Number W12HZ2020009 to P.R. and P.H. We thank Sue Stuska (National Park Service) and Rudi Rudolph (Carteret County) for their help and support with coordinating field surveys to Cape Lookout National Seashore and Bogue Banks. Sarah

Spiegler (North Carolina Sea Grant) helped organize and host stakeholder meetings. We are grateful to all the volunteers who were instrumental in field campaigns, including Jeffrey Wood, Crystal Wasley, Rebecca Mostow, Ian Reeves, Elsemarie Mullins, Hannah Lawrence, John Stepanek, Caitlin Magel, Nicholas Cohn, Evan Goldstein, Katherine Anarde, and Reuben Biel. Hannah Lawrence and Megan Andreasen helped with sediment sieving. Finally, we thank Nicholas Cohn (Deltares USA, Inc) for his guidance with the Windsurf modeling.

References

Arens, S.M., Baas, A.C.W., Boxel, J.H. Van, Kalkman, C., 2001. Influence of Reed Stem Density on Foredune Development. Earth Surf Process Landf 26, 1161–1176. https://doi.org/10.1002/esp.257

Bagnold, R.A., 1941. The Physics of Blown Sand and Desert Dunes. Methnen, London.

Barbier, E.B., Hacker, S.D., Kennedy, C., Koch, E.W., Stier, A.C., Silliman, B.R., 2011. The value of estuarine and coastal ecosystem services. Ecol Monogr 81, 169–193. https://doi.org/10.1890/10-1510.1

Bauer, B.O., Davidson-Arnott, R.G.D., 2003. A general framework for modeling sediment supply to coastal dunes including wind angle, beach geometry, and fetch effects. Geomorphology 49, 89–108.

Bauer, B.O., Davidson-Arnott, R.G.D., Hesp, P.A., Namikas, S.L., Ollerhead, J., Walker, I.J., 2009. Aeolian sediment transport on a beach: Surface moisture, wind fetch, and mean transport. Geomorphology 105, 106–116.

Bauer, B.O., Davidson-Arnott, R.G.D., Nordstrom, K.F., Ollerhead, J., Jackson, N.L., 1996. Indeterminacy in aeolian sediment transport across beaches. J Coast Res 641–653.

Belly, P.Y., 1964. Sand Movement by Wind. Washington DC.

Biel, R.G., Hacker, S.D., Ruggiero, P., 2019. Elucidating Coastal Foredune Ecomorphodynamics in the U.S. Pacific Northwest via Bayesian Networks. J Geophys Res Earth Surf 124, 1919–1938. https://doi.org/10.1029/2018JF004758

Bonte, D., Batsleer, F., Provoost, S., Reijers, V., Vandegehuchte, M.L., van de Walle, R., Dan, S., Matheve, H., Rauwoens, P., Strypsteen, G., 2021. Biomorphogenic feedbacks and the spatial organization of a dominant grass steer dune development. Front Ecol Evol 9.

Bryant, D.B., Anderson Bryant, M., Sharp, J.A., Bell, G.L., Moore, C., 2019. The response of vegetated dunes to wave attack. Coastal Engineering 152, 103506. https://doi.org/https://doi.org/10.1016/j.coastaleng.2019.103506

Carter, R.W.G., 1976. Formation, maintenance and geomorphological significance of an aeolian shell pavement. Journal of Sedimentary Research 46, 418–429.

Carter, R.W.G., Rihan, C.L., 1978. Shell and pebble pavements on beaches: Examples from the north coast of Ireland. Catena (Amst) 5, 365–374. https://doi.org/https://doi.org/10.1016/0341-8162(78)90019-X

Castelle, B., Bujan, S., Ferreira, S., Dodet, G., 2017. Foredune morphological changes and beach recovery from the extreme 2013 / 2014 winter at a high-energy sandy coast. Mar Geol 385, 41–55. https://doi.org/10.1016/j.margeo.2016.12.006

Castelle, B., Marieu, V., Bujan, S., 2019. Alongshore-Variable Beach and Dune Changes on the Timescales from Days (Storms) to Decades Along the Rip-dominated Beaches of the Gironde Coast, SW France. J Coast Res. https://doi.org/10.2112/SI88-012.1

Charbonneau, B.R., Casper, B.B., 2018. Wind tunnel tests inform Ammophila planting spacing for dune management. https://doi.org/https://doi.org/10.31223/osf.io/aeuhb

Charbonneau, B.R., Dohner, S.M., Wnek, J.P., Barber, D., Zarnetske, P., Casper, B.B., 2021. Vegetation effects on coastal foredune initiation: Wind tunnel experiments and field validation for three dune-building plants. Geomorphology 378, 107594. https://doi.org/https://doi.org/10.1016/j.geomorph.2021.107594

Charbonneau, B.R., Duarte, A., Swannack, T.M., Johnson, B.D., Piercy, C.D., 2022. DOONIES: A process-based ecogeomorphological functional community model for coastal dune vegetation and landscape dynamics. Geomorphology 398. https://doi.org/10.1016/J.GEOMORPH.2021.108037

Charbonneau, B.R., Wooton, L.S., Wnek, J.P., Langley, J.A., Posner, M.A., 2017. A species effect on storm erosion: Invasive sedge stabilized dunes more than native grass during Hurricane Sandy. Journal of Applied Ecology 54, 1385–1394. https://doi.org/10.1111/1365-2664.12846

Cohn, N., Brodie, K.L., Johnson, B., Palmsten, M.L., 2021. Hotspot dune erosion on an intermediate beach. Coastal Engineering 170. https://doi.org/10.1016/J.COASTALENG.2021.103998

Cohn, N., Hoonhout, B., Goldstein, E., de Vries, S., Moore, L., Durán Vinent, O., Ruggiero, P., 2019a. Exploring Marine and Aeolian Controls on Coastal Foredune

Growth Using a Coupled Numerical Model. J Mar Sci Eng 7, 13. https://doi.org/10.3390/jmse7010013

Cohn, N., Ruggiero, P., de Vries, S., Kaminsky, G., 2018. New Insights on Coastal Foredune Growth: The Relative Contributions of Marine and Aeolian Processes. Geophys Res Lett 45, 4965–4973. https://doi.org/10.1029/2018GL077836

Cohn, N., Ruggiero, P., Garcia-Medina, G., Anderson, D., Serafin, K.A., Biel, R.G., 2019b. Environmental and morphologic controls on wave-induced dune response. Geomorphology 329, 108–128.

Corenblit, D., Baas, A.C.W., Bornette, G., Darrozes, J., Delmotte, S., Francis, R.A., Gurnell, A.M., Julien, F., Naiman, R.J., Steiger, J., 2011. Feedbacks between geomorphology and biota controlling Earth surface processes and landforms: A review of foundation concepts and current understandings. Earth Science Reviews 106, 307–331. https://doi.org/10.1016/j.earscirev.2011.03.002

Crapoulet, A., Héquette, A., Marin, D., Levoy, F., Bretel, P., 2017. Variations in the response of the dune coast of northern France to major storms as a function of available beach sediment volume. Earth Surf Process Landf 42, 1603–1622.

Davidson-Arnott, R., Hesp, P.A., Ollerhead, J., Walker, I., Bauer, B., Delgado-Fernandez, I., Smyth, T., 2018. Sediment budget controls on foredune height: Comparing simulation model results with field data. Earth Surf Process Landf 43, 1798–1810. https://doi.org/10.1002/esp.4354

Delgado-Fernandez, I., Davidson-Arnott, R., 2011. Meso-scale aeolian sediment input to coastal dunes : The nature of aeolian transport events. Geomorphology 126, 217–232. https://doi.org/10.1016/j.geomorph.2010.11.005

Dolan, R., Lins, H., 1985. The Outer Banks of North Carolina. Washington DC.

Du, J., Hesp, P.A., 2020. Salt Spray Distribution and Its Impact on Vegetation Zonation on Coastal Dunes: a Review. Estuaries and Coasts 43, 1885–1907.

Durán, O., Moore, L.J., 2013. Vegetation controls on the maximum size of coastal dunes. PNAS 10, 17217–17222. https://doi.org/10.1073/pnas.1307580110

Esler, A.E., 1970. Manawatu sand dune vegetation, in: Proceedings (New Zealand Ecological Society. New Zealand Ecological Society, pp. 41–46.

Fabbri, S., Giambastiani, B.M.S., Sistilli, F., Scarelli, F., Gabbianelli, G., 2017. Geomorphological analysis and classification of foredune ridges based on Terrestrial Laser Scanning (TLS) technology. Geomorphology 295, 436–451. https://doi.org/10.1016/j.geomorph.2017.08.003

Feagin, R.A., Figlus, J., Zinnert, J.C., Sigren, J., Martínez, M.L., Silva, R., Smith, W.K., Cox, D., Young, D.R., Carter, G., 2015. Going with the flow or against the grain? The promise of vegetation for protecting beaches, dunes, and barrier islands from erosion. Front Ecol Environ 13, 203–210.

Field, J., Pelletier, J., 2018. Controls on the aerodynamic roughness length and the grain-size dependence of aeolian sediment transport. Earth Surf Process Landf 43, 2616–2626. https://doi.org/10.1002/esp.4420

Folk, R.L., 1968. Petrography of sedimentary rocks. Hemphill’s Bookstore, Austin, TX.

Folk, R.L., Ward, W., 1957. Brazos River bar: A study in the significance of grain size parameters. J Sediment Petrol 27, 3–26.

Godfrey, P.J., 1977. Climate, plant response and development of dunes on barrier beaches along the U.S. east coast. Int J Biometeorol 21, 203–216. https://doi.org/10.1007/BF01552874

Godfrey, P.J., 1976. Barrier Island Ecology of Cape Lookout National Seashore and Vicinity, North Carolina. National Park Service.

Goldsmith, V., 1978. Coastal Dunes, in: Coastal Sedimentary Environments. Springer, New York. https://doi.org/https://doi.org/10.1007/978-1-4684-0056-4_5

Goldstein, E.B., Moore, L.J., 2018. A calibration workflow for coastal dune models [WWW Document]. https://doi.org/10.31223/osf.io/cd87u

Goldstein, E.B., Moore, L.J., Vinent, O.D., 2017. Lateral vegetation growth rates exert control on coastal foredune " hummockiness " and coalescing time. Earth Surface Dynamics 5, 417–427.

Goldstein, E.B., Mullins, E. v., Moore, L.J., Biel, R.G., Brown, J.K., Hacker, S.D., Jay, K.R., Mostow, R.S., Ruggiero, P., Zinnert, J.C., 2018. Literature-based latitudinal distribution and possible range shifts of two US east coast dune grass species (Uniola paniculata and Ammophila breviligulata). PeerJ 6. https://doi.org/10.7717/peerj.4932

Gomes da Silva, P., Coco, G., Garnier, R., Klein, A.H.F., 2020. On the prediction of runup, setup and swash on beaches. Earth Sci Rev 204, 103148. https://doi.org/https://doi.org/10.1016/j.earscirev.2020.103148

Gracia, A., Rangel-Buitrago, N., Oakley, J.A., Williams, A.T., 2018. Use of ecosystems in coastal erosion management. Ocean Coast Manag 156, 277–289. https://doi.org/10.1016/j.ocecoaman.2017.07.009

Hacker, S.D., Jay, K.R., Cohn, N., Goldstein, E.B., Hovenga, P.A., Itzkin, M., Moore, L.J., Mostow, R.S., Mullins, E. v, Ruggiero, P., 2019. Species-Specific Functional Morphology of Four US Atlantic Coast Dune Grasses : Biogeographic Implications for Dune Shape and Coastal Protection. Diversity (Basel) 11, 82.

Hacker, S.D., Zarnetske, P., Seabloom, E., Ruggiero, P., Mull, J., Gerrity, S., Jones, C., 2012. Subtle differences in two non-native congeneric beach grasses significantly affect their colonization, spread, and impact. Oikos 121, 138–148. https://doi.org/10.1111/j.1600-0706.2011.18887.x

Héquette, A., Ruz, M.-H., Zemmour, A., Marin, D., Cartier, A., Sipka, V., 2019. Alongshore variability in coastal dune erosion and post-storm recovery, northern coast of France. J Coast Res 88, 25–45.

Hesp, P.A., 1989. A review of biological and geomorphological processes involved in the initiation and development of incipient foredunes. Proceedings of the Royal Society of Edinburgh, Section B: Biological Sciences 96, 181–201.

Hesp, P.A., 1988. Surfzone, beach, and foredune interactions on the Australian South East Coast. J Coast Res 15–25.

Hesp, P.A., Dong, Y., Cheng, H., Booth, J.L., 2019. Wind flow and sedimentation in artificial vegetation: Field and wind tunnel experiments. Geomorphology 337, 165–182. https://doi.org/10.1016/j.geomorph.2019.03.020

Hesp, P.A., Smyth, T.A.G., 2016. Surfzone-Beach-Dune interactions: Flow and Sediment Transport across the Intertidal Beach and Backshore. J Coast Res 75, 8–12. https://doi.org/10.2112/SI75-002.1

Holman, R.A., Sallenger Jr., A.H., 1985. Setup and swash on a natural beach. J Geophys Res Oceans 90, 945–953.

Hong, C., Weiwei, H., Chenchen, L., Xueyong, Z., Liqiang, K., Tianle, C., Kaidi, Z., 2019. Transition model for air fl ow fi elds from single plants to multiple plants. Agric For Meteorol 266–267, 29–42. https://doi.org/10.1016/j.agrformet.2018.11.039

Hoonhout, B., 2020. AeoLiS Documentation. https://doi.org/https://aeolis.readthedocs.io/_/downloads/en/latest/pdf/

Hoonhout, B.M., de Vries, S., 2016. A process-based model for aeolian sediment transport and spatiotemporal varying sediment availability. J Geophys Res Earth Surf 121, 1555–1575. https://doi.org/10.1002/2015JF003692

Houser, C., 2013. Alongshore variation in the morphology of coastal dunes: Implications for storm response. Geomorphology 199, 48–61. https://doi.org/10.1016/J.GEOMORPH.2012.10.035

Houser, C., Hapke, C., Hamilton, S., 2008. Controls on coastal dune morphology, shoreline erosion and barrier island response to extreme storms. Geomorphology 100, 223–240. https://doi.org/https://doi.org/10.1016/j.geomorph.2007.12.007

Hovenga, P.A., Ruggiero, P., Cohn, N., Jay, K.R., Hacker, S.D., Itzkin, M., Moore, L.J., 2019. Drivers of Dune Evolution in Cape Lookout National Seashore, Nc, in: Coastal Sediments 2019. pp. 1283–1296. https://doi.org/10.1142/9789811204487_0112

Hovenga, P.A., Ruggiero, P., Goldstein, E.B., Moore, L.J., Hacker, S.D., 2021. The relative role of constructive and destructive processes in dune evolution on Cape Lookout National Seashore, North Carolina, USA. Earth Surf Process Landf.

Itzkin, M., Moore, L.J., Ruggiero, P., Hovenga, P.A., Hacker, S.D., 2022. Combining process-based and data-driven approaches to forecast beach and dune change. Environmental Modelling & Software 153. https://doi.org/10.1016/J.ENVSOFT.2022.105404

Jackson, D.W.T., Beyers, M., Delgado-Fernandez, I., Baas, A.C.W., Cooper, A.J., Lynch, K., 2013. Airflow reversal and alternating corkscrew vortices in foredune wake zones during perpendicular and oblique offshore winds. Geomorphology 187, 86–93. https://doi.org/https://doi.org/10.1016/j.geomorph.2012.12.037

Jackson, P.S., Hunt, J.C.R., 1975. Turbulent wind flow over a low hill. Quarterly Journal of the Royal Meteorological Society 101, 929–955.

Jay, K.R., Hacker, S.D., Hovenga, P.A., Moore, L.J., Ruggiero, P., 2022. Sand supply and dune grass species density affect foredune shape along the US Central Atlantic Coast. Ecosphere.

Keijsers, J.G.S., Groot, A.V. de, Riksen, M.J.P.M., 2016. Modeling the biogeomorphic evolution of coastal dunes. J Geophys Res Earth Surf 121, 1161–1181. https://doi.org/10.1002/2015JF003815.Abstract

Komar, P.D., Allan, J., Guillermo, M.D., Marra, J.J., Ruggiero, P., 2001. El Nino and La Nina : Erosion Processes and Impacts, in: Coastal Engineering 2000. pp. 2414–2427.

Larson, M., Erikson, L., Hanson, H., 2004. An analytical model to predict dune erosion due to wave impact. Coastal engineering 51, 675–696.

Lentz, E.E., Hapke, C.J., 2019. Geologic framework influences on the geomorphology of an anthropogenically modified barrier island: Assessment of dune/beach changes at Fire Island, New York. Geomorphology 126, 82–96. https://doi.org/10.1016/j.geomorph.2010.10.032

Levin, N., Kidron, G.J., BEN-DOR, E., 2008. A field quantification of coastal dune perennial plants as indicators of surface stability, erosion or deposition. Sedimentology 55, 751–772.

Liu, C., Zheng, Z., Cheng, H., Zou, X., 2018. Airflow around single and multiple plants. Agric For Meteorol 252, 27–38. https://doi.org/10.1016/j.agrformet.2018.01.009

Martínez, M.L., Psuty, N.P., 2004. Coastal Dunes. Springer Verlag.

Masselink, G., Scott, T., Poate, T., Russell, P., Davidson, M., Conley, D., 2016. The extreme 2013 / 2014 winter storms : hydrodynamic forcing and coastal response along the southwest coast of England. Earth Surf Process Landf 391, 378–391. https://doi.org/10.1002/esp.3836

Maun, M.A., 2009. The biology of coastal sand dunes. Oxford University Press.

McKenna Neuman, C., Li, B., Nash, D., 2012. Micro-topographic analysis of shell pavements formed by aeolian transport in a wind tunnel simulation. J Geophys Res Earth Surf 117.

Miot da Silva, G., Hesp, P.A., 2010. Coastline orientation, aeolian sediment transport and foredune and dunefield dynamics of Moçambique Beach, Southern Brazil. Geomorphology 120, 258–278.

Miot da Silva, G., Hesp, P.A., Peixoto, J., Dillenburg, S.R., 2008. Foredune vegetation patterns and alongshore environmental gradients: Mocambique beach, Santa Catarina Island, Brazil. Earth Surface Processes and Landforms: The Journal of the British Geomorphological Research Group 33, 1557–1573.

Miot da Silva, G., Mostafa Siadat Mousavi, S., Jose, F., 2012. Wave-driven sediment transport and beach-dune dynamics in a headland bay beach. Mar Geol 323–325, 29–46. https://doi.org/10.1016/j.margeo.2012.07.015

Moulton, M.A.B., Hesp, P.A., Miot da Silva, G., Keane, R., Fernandez, G.B., 2021. Surfzone-beach-dune interactions along a variable low wave energy dissipative beach. Mar Geol 435, 106438. https://doi.org/https://doi.org/10.1016/j.margeo.2021.106438

Mullins, E., Moore, L.J., Goldstein, E.B., Jass, T., Bruno, J., Durán Vinent, O., 2019. Investigating dune-building feedback at the plant level: Insights from a multispecies field experiment. Earth Surf Process Landf 44, 1734–1747.

Murphy, A.H., Epstein, E.S., 1989. Skill scores and correlation coefficients in model verification. Mon Weather Rev 117, 572–582.

NOAA, 2020a. Tide & Currents: Beaufort, Dune Marine Lab, NC - Station ID: 8656483 [WWW Document]. URL https://tidesandcurrents.noaa.gov/stationhome.html?id=8656483

NOAA, 2020b. National Data Buoy Center Station: CLKN7 - Cape Lookout, NC [WWW Document]. URL https://www.ndbc.noaa.gov/station_page.php?station=clkn7

NOAA, 2018. Digital Coast Historical Hurricane Tracks [WWW Document]. URL https://coast.noaa.gov/hurricanes/

NOAA, 2016. Digital Coast Data Access Viewer [WWW Document]. URL https://coast.noaa.gov/dataviewer/#/lidar/search/

Nordstrom, K.F., Lotstein, E.L., Review, S.G., Jan, N., 1989. Perspectives on Resource Use of Dynamic Coastal Dunes. Geogr Rev 79, 1–12.

Olson, J., 1958a. Lake Michigan dune development 1. Wind-velocity profiles. J Geol 66, 254–263.

Olson, J., 1958b. Lake Michigan dune development 2. Plants as agents and tools in geomorphology. J Geol 66.

Passeri, D.L., Bilskie, M. v, Plant, N.G., Long, J.W., Hagen, S.C., 2018. Dynamic modeling of barrier island response to hurricane storm surge under future sea level rise. Clim Change 149, 413–425.

Passeri, D.L., Dalyander, P.S., Long, J.W., Mickey, R.C., Jenkins III, R.L., Thompson, D.M., Plant, N.G., Godsey, E.S., Gonzalez, V.M., 2020. The roles of storminess and sea level rise in decadal barrier island evolution. Geophys Res Lett 47, e2020GL089370.

Pellón, E., de Almeida, L.R., González, M., Medina, R., 2020. Relationship between foredune profile morphology and aeolian and marine dynamics: A conceptual model. Geomorphology 351, 106984. https://doi.org/https://doi.org/10.1016/j.geomorph.2019.106984

Pettijohn, F.J., Potter, P.E., Siever, R., 1987. Sand and Sandstone. Springer-Verlag, New York.

Psuty, N.P., 1988. Sediment budget and dune/beach interaction. J Coast Res 1–4.

Rafati, Y., Hsu, T.-J., Elgar, S., Raubenheimer, B., Quataert, E., van Dongeren, A., 2021. Modeling the hydrodynamics and morphodynamics of sandbar migration events. Coastal Engineering 166, 103885.

Riggs, S.R., Ames, D. V., 2007. Effect of Storms on Barrier Island Dynamics, Cape Lookout National Seashore, North Carolina, 1960–2001. Reston.

Roelvink, D., Costas, S., 2019. Coupling nearshore and aeolian processes: XBeach and duna process-based models. Environmental Modelling and Software 115, 98–112. https://doi.org/10.1016/j.envsoft.2019.02.010

Roelvink, D., Reniers, A., van Dongeren, A., van Thiel de Vries, J., McCall, R., Lescinski, J., 2009. Modelling storm impacts on beaches, dunes and barrier islands. Coastal Engineering 56, 1133–1152. https://doi.org/10.1016/j.coastaleng.2009.08.006

Ruggiero, P., Cohn, N., Hoonhout, B., Goldstein, E., de Vries, S., Moore, L., Hacker, S.D., Durán Vinent, O., 2019. Simulating dune evolution on managed coastlines: Exploring management options with the Coastal Recovery from Storms Tool (CReST). Shore and Beach 87, 36–43.

Ruggiero, P., Kaminsky, G.M., Gelfenbaum, G., Voigt, B., 2005. Seasonal to Interannual Morphodynamics along a High-Energy Dissipative Littoral Cell. J Coast Res 21, 553–578. https://doi.org/10.2112/03-0029.1

Ruggiero, P., Komar, P.D., McDougal, W.G., Marra, J.J., Beach, R.A., 2001. Wave Runup, Extreme Water Levels and the Erosion of Properties Backing Beaches. J Coast Res 17, 407–419.

Sallenger, A.H., 2000. Storm Impact Scale for Barrier Islands. J Coast Res 16, 890–895. https://doi.org/10.2307/4300099

Saye, S.E., van der Wal, D., Pye, K., Blott, S.J., 2005. Beach–dune morphological relationships and erosion/accretion: an investigation at five sites in England and Wales using LIDAR data. Geomorphology 72, 128–155.

Seabloom, E.W., Ruggiero, P., Hacker, S.D., Mull, J., Zarnetske, P., 2013. Invasive grasses, climate change, and exposure to storm-wave overtopping in coastal dune ecosystems. Glob Chang Biol 19, 824–832. https://doi.org/10.1111/gcb.12078

Seneca, E.D., 1972. Seedling response to salinity in four dune grasses from the Outer Banks of North Carolina. Ecology 53, 465–471.

Serafin, K.A., Ruggiero, P., Barnard, P.L., Stockdon, H.F., 2019. The influence of shelf bathymetry and beach topography on extreme total water levels: Linking large-scale changes of the wave climate to local coastal hazards. Coastal Engineering 150, 1–17. https://doi.org/https://doi.org/10.1016/j.coastaleng.2019.03.012

Sherman, D.J., Bauer, B.O., 1993. Dynamics of beach-dune systems. Prog Phys Geogr 17, 413–447.

Short, A.D., Hesp, P.A., 1982. Wave, beach and dune interactions in southeastern Australia. Mar Geol 48, 259–284. https://doi.org/10.1016/0025-3227(82)90100-1

Splinter, K.D., Kearney, E.T., Turner, I.L., 2018. Drivers of alongshore variable dune erosion during a storm event: Observations and modelling. Coastal Engineering 131, 31–41. https://doi.org/10.1016/j.coastaleng.2017.10.011

Stockdon, H.F., Holman, R.A., Howd, P.A., Sallenger, A.H., 2006. Empirical parameterization of setup, swash, and runup. Coastal Engineering 53, 573–588.

Stockdon, H.F., Thompson, D.M., 2007. Vulnerability of National Park Service Beaches to Inundation during a Direct Hurricane Landfall: Cape Lookout National Seashore. St. Petersburg.

Sudmeier-Rieux, K., Nehren, U., Sandholz, S., Doswald, N., 2019. Disasters and Ecosystems, Resilience in a Changing Climate - Source Book. United Nations Environment Programme, Geneva. https://doi.org/10.5281/zenodo.3493377

Sutherland, J., Peet, A.H., Soulsby, R.L., 2004. Evaluating the performance of morphological models. Coastal Engineering 51, 917–939. https://doi.org/10.1016/J.COASTALENG.2004.07.015

Theuerkauf, E.J., Rodriguez, A.B., Fegley, S.R., Luettich Jr, R.A., 2014. Sea level anomalies exacerbate beach erosion. Geophys Res Lett 41, 5139–5147.

U.S. Army Corps. of Engineers, 1997. Available WIS Stations - Atlantic.

Walker, I., Hesp, P.A., 2013. Fundamentals of aeolian sediment transport: airflow over dunes. Treatise on geomorphology 3, 109–133.

Walker, I.J., 2020. Aeolian (windblown) sand transport over beaches, in: Sandy Beach Morphodynamics. Elsevier, pp. 213–253.

Weng, W.S., Hunt, J.C.R., Carruthers, D.J., Warren, A., Wiggs, G.F.S., Livingstone, I., Castro, I., 1991. Air flow and sand transport over sand-dunes, in: Aeolian Grain Transport. Springer, pp. 1–22.

White, B.R., Tsoar, H., 1998. Slope effect on saltation over a climbing sand dune. Geomorphology 22, 159–180.

Wolner, C.W. v, Moore, L.J., Young, D.R., Brantley, S.T., Bissett, S.N., Mcbride, R.A., 2013. Ecomorphodynamic feedbacks and barrier island response to disturbance: Insights from the Virginia Barrier Islands, Mid-Atlantic Bight, USA. Geomorphology 199, 115–128. https://doi.org/10.1016/j.geomorph.2013.03.035

Woodhouse, W.W., 1978. Dune building and stabilization with vegetation. The Center.

Yousefi Lalimi, F., Silvestri, S., Moore, L.J., Marani, M., 2017. Coupled topographic and vegetation patterns in coastal dunes: Remote sensing observations and ecomorphodynamic implications. J Geophys Res Biogeosci 122, 119–130. https://doi.org/10.1002/2016JG003540

Zarnetske, P.L., Hacker, S.D., Seabloom, E.W., Ruggiero, P., Killian, J.R., Maddux, T.B., Cox, D., 2012. Biophysical feedback mediates effects of invasive grasses on coastal dune shape. Ecology 93, 1439–1450.

Zarnetske, P.L., Ruggiero, P., Seabloom, E.W., Hacker, S.D., 2015. Coastal foredune evolution: the relative influence of vegetation and sand supply in the US Pacific Northwest. J R Soc Interface 12.